Limitations from LHC RF Fingers

Presenters: Chiara Antuono and Patrick Krkotić

G. Bregliozzi, S. Calatroni, E. De La Fuente, A. Galloro, B. Salvant, L. Sito, C. Zannini

Joint Accelerator Performance Workshop, 6 December 2023

Contents

Fault recording in 2023

May 25-26, 2023: Pressure spikes within the vacuum sector **A4L1** during the fill ID 8828 (**$1.63 \cdot 10^{11}$ p/b – 2358 bunches**) lead to a beam dump due to losses.

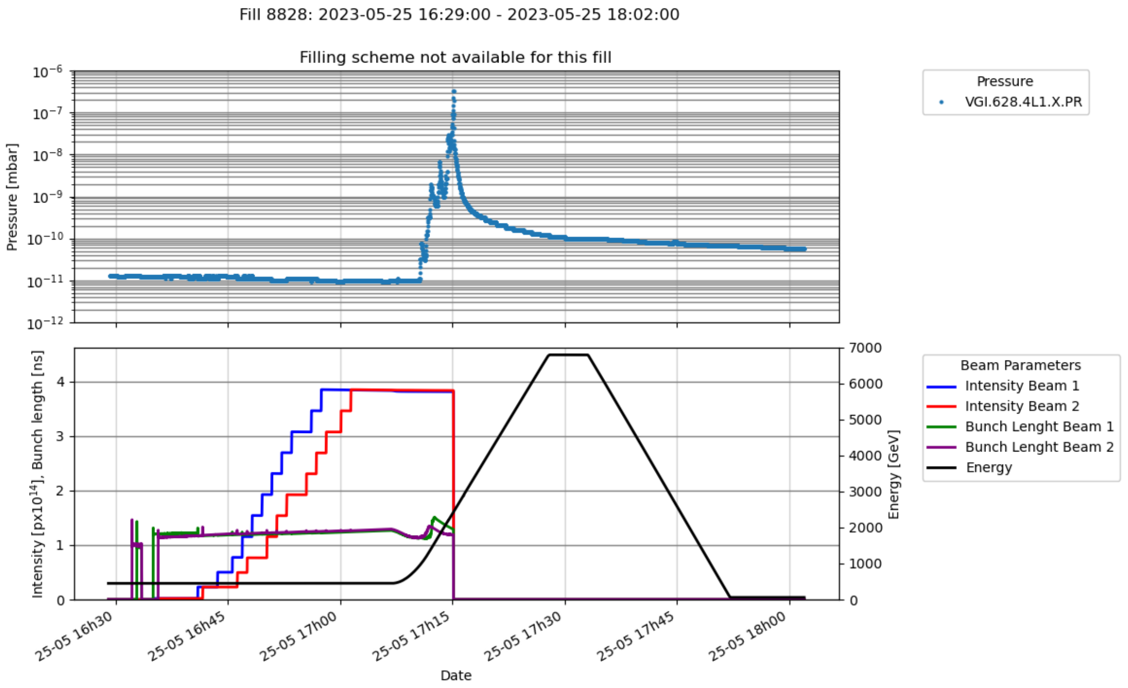

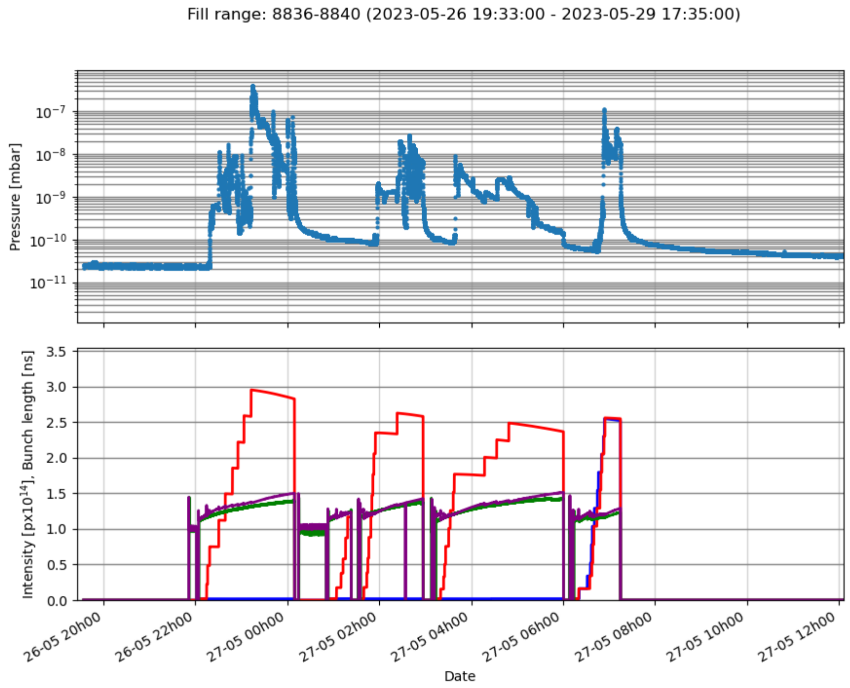

Fault recording in 2023

ID212.7 RF Finger Module

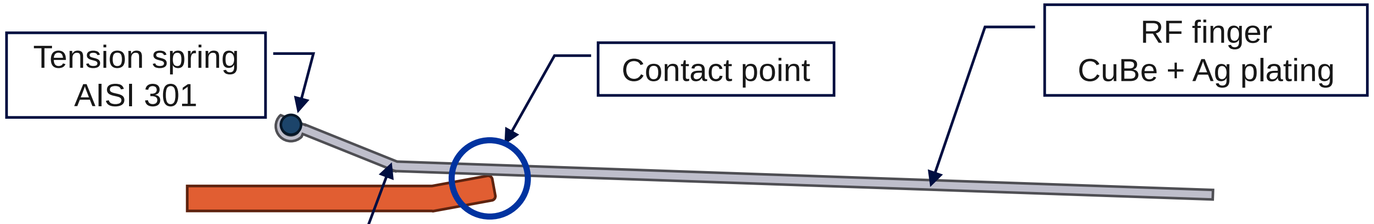

Spring ensures the electrical contact between fingers/transition tube

Type of module :
Circular
Standard RF Finger
Aperture ϕ212.7 mm
Installation length
400 mm

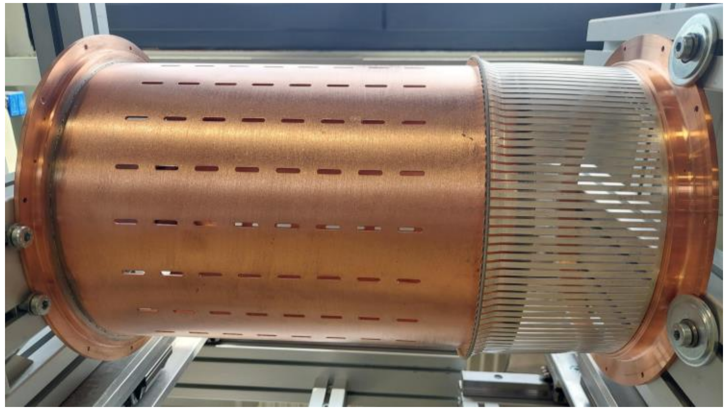

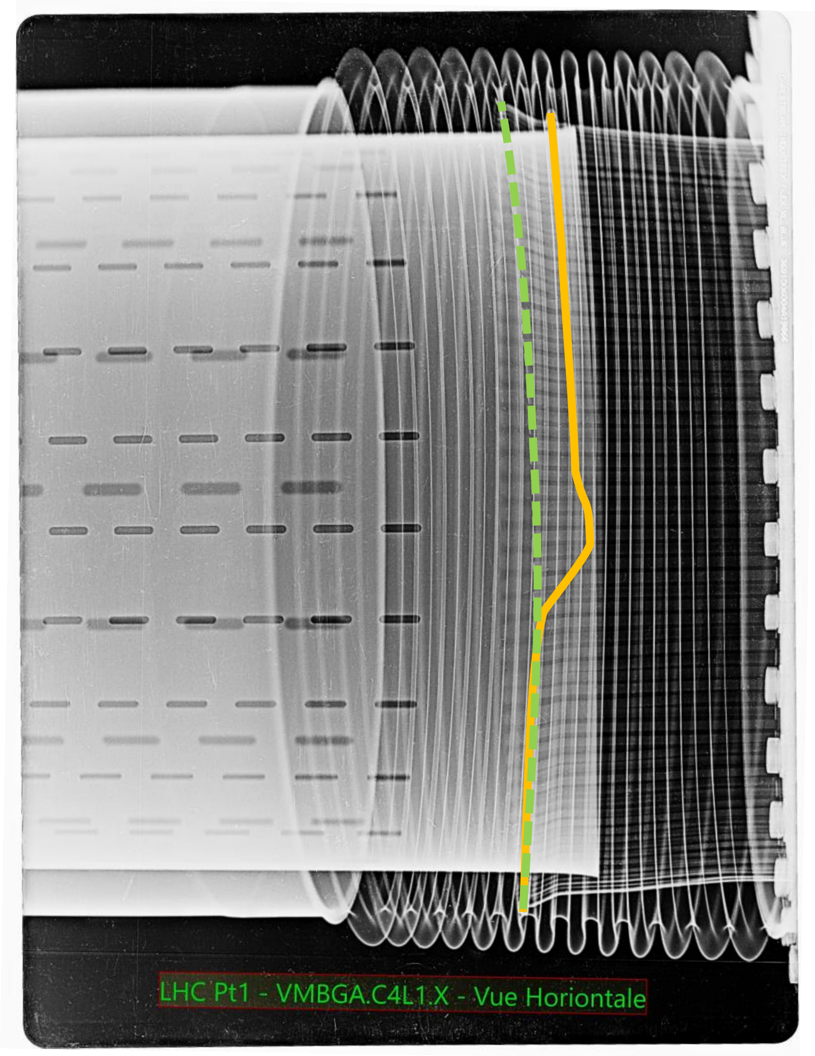

Fault recording in 2023

Visual inspection:

- annealed/plasticised spring → localized temperature increase to more than 500°C
- localised extremely high temperature producing debris, sputtering and sublimation of austenitic stainless-steel spring
- cascade of failure with consequent loss of electrical contact of RF fingers on the transition tube perimeter

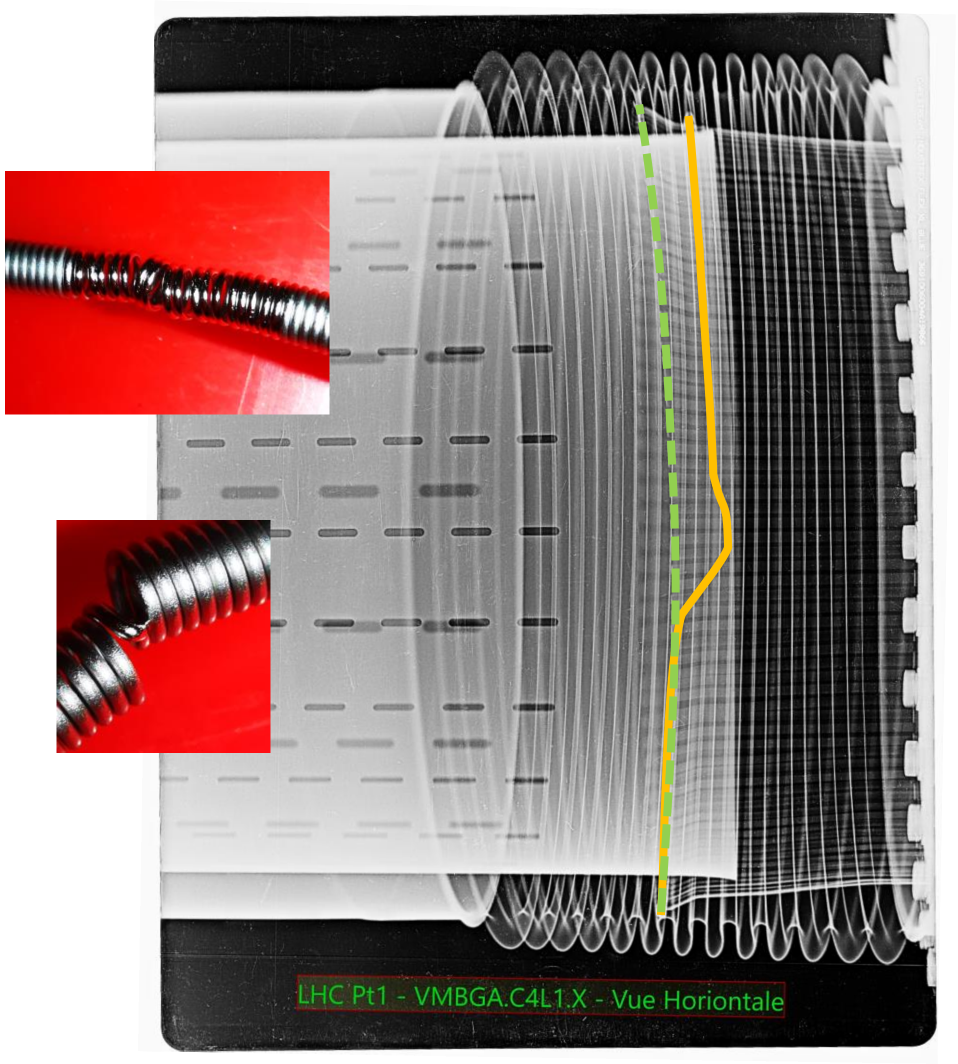

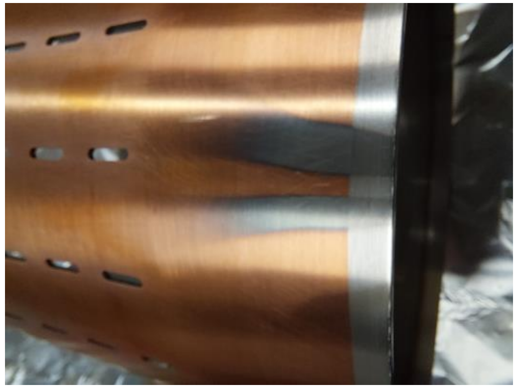

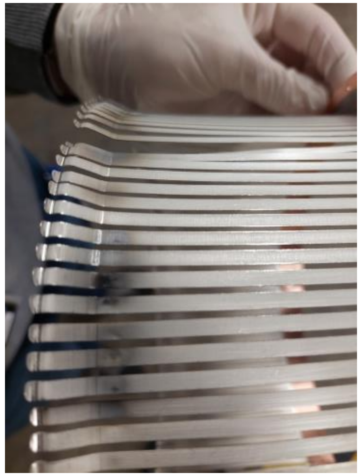

X-ray investigation

Inspection of all 71 modules present in the LHC machine

- 1 failed, 8 degraded

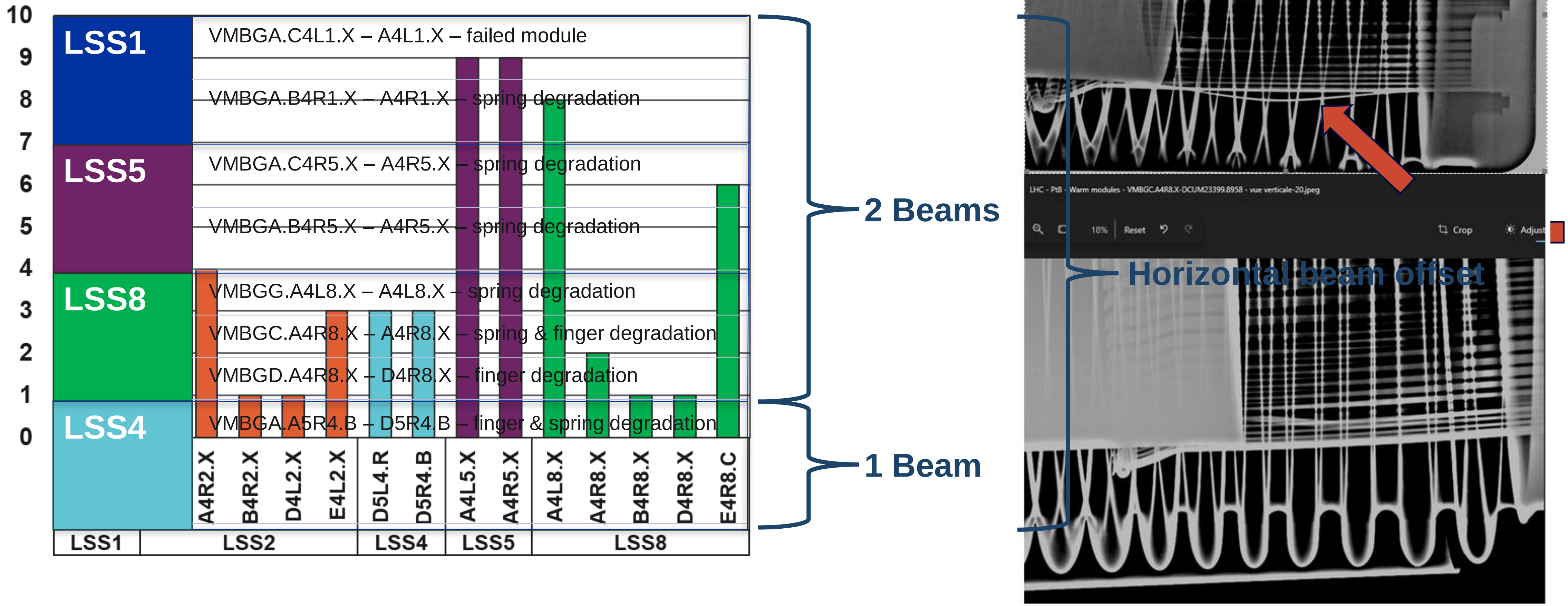

02

Understanding of the Failure

Material and Production Analysis

Tension spring properties

Stainless Steel 1.4310
AISI 301 (X10CrNi18-8)

Good mechanical properties and corrosion resistance

- The material can theoretically be used up to +250°C

Effects of the bake-out cycle: elasticity of the spring versus different elongations **(EDMS)**

- As received: compatible with specifications
- **8 days 250°C** bake out: no degradation
- **8 days 330°C** bake out: removal of pre-load and length increase

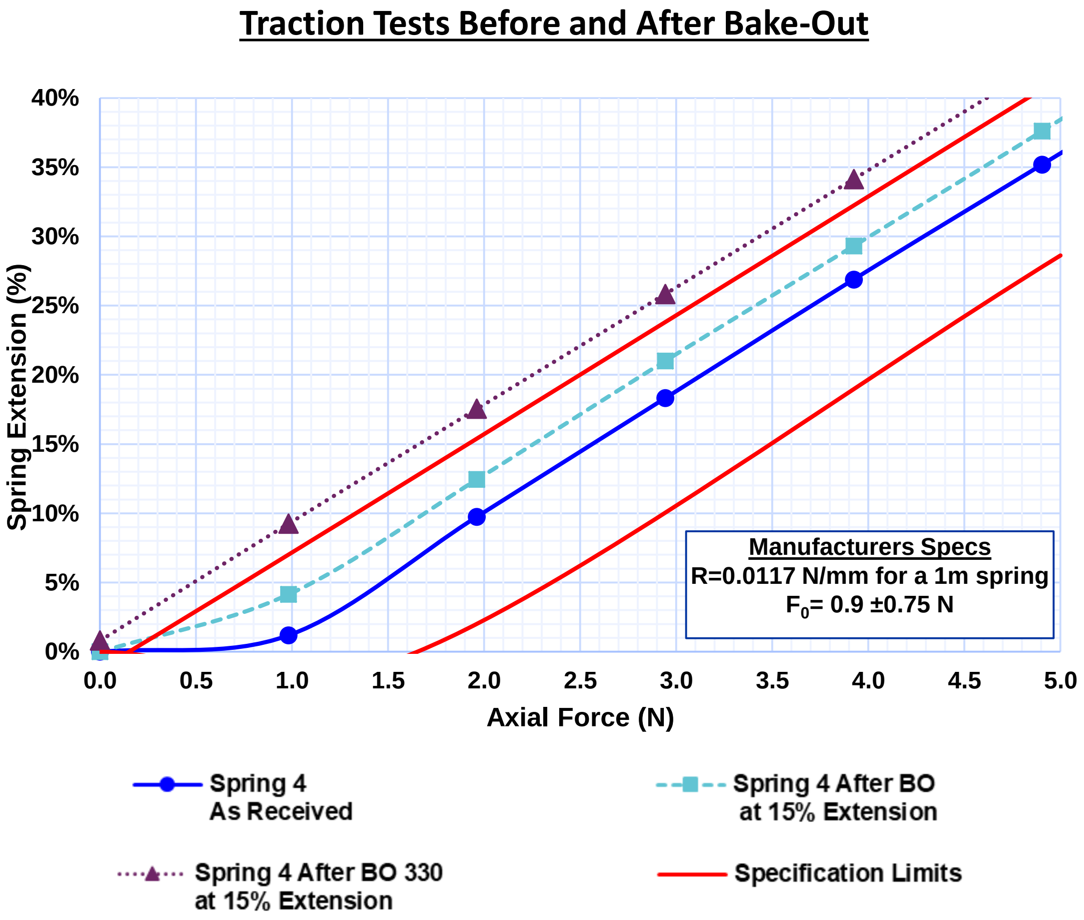

Thermal simulations

- Visual inspection and radiography indicate that heating of the spring is the triggering mechanism of the first module failure
- Finite Element Method simulations via COMSOL were conducted to determine the power deposition necessary to heat the spring in a steady state **(EDMS)**

uniform power distribution

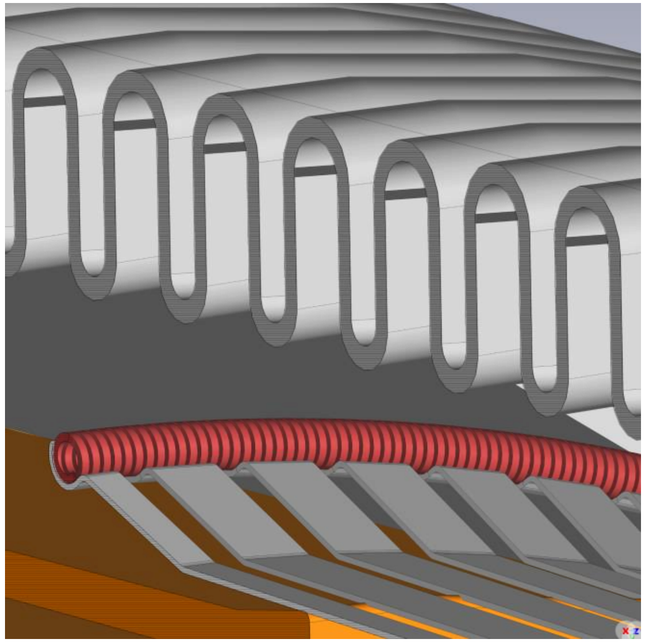

localised power

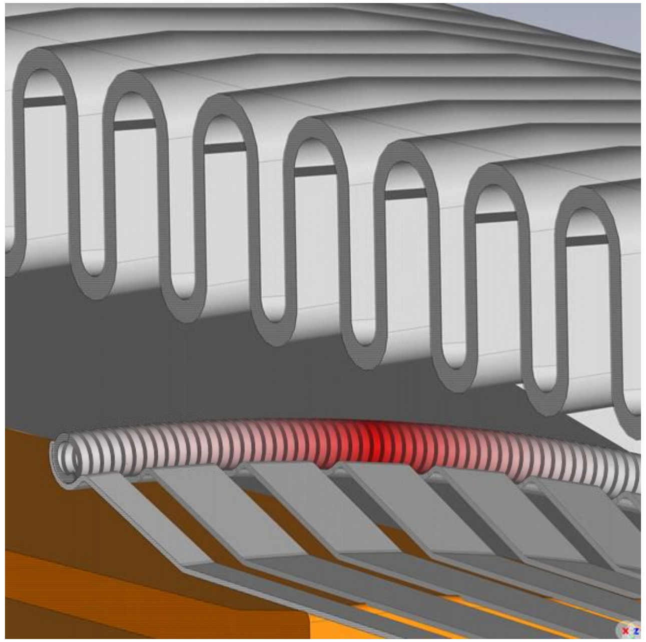

Thermal simulations

- Visual inspection and radiography indicate that heating of the spring is the triggering mechanism of the first module failure
- Finite Element Method simulations via COMSOL were conducted to determine the power deposition necessary to heat the spring in a steady state **(EDMS)**

Annealing condition of the spring: annealing/plasticisation of the spring at a temperature of 500°C

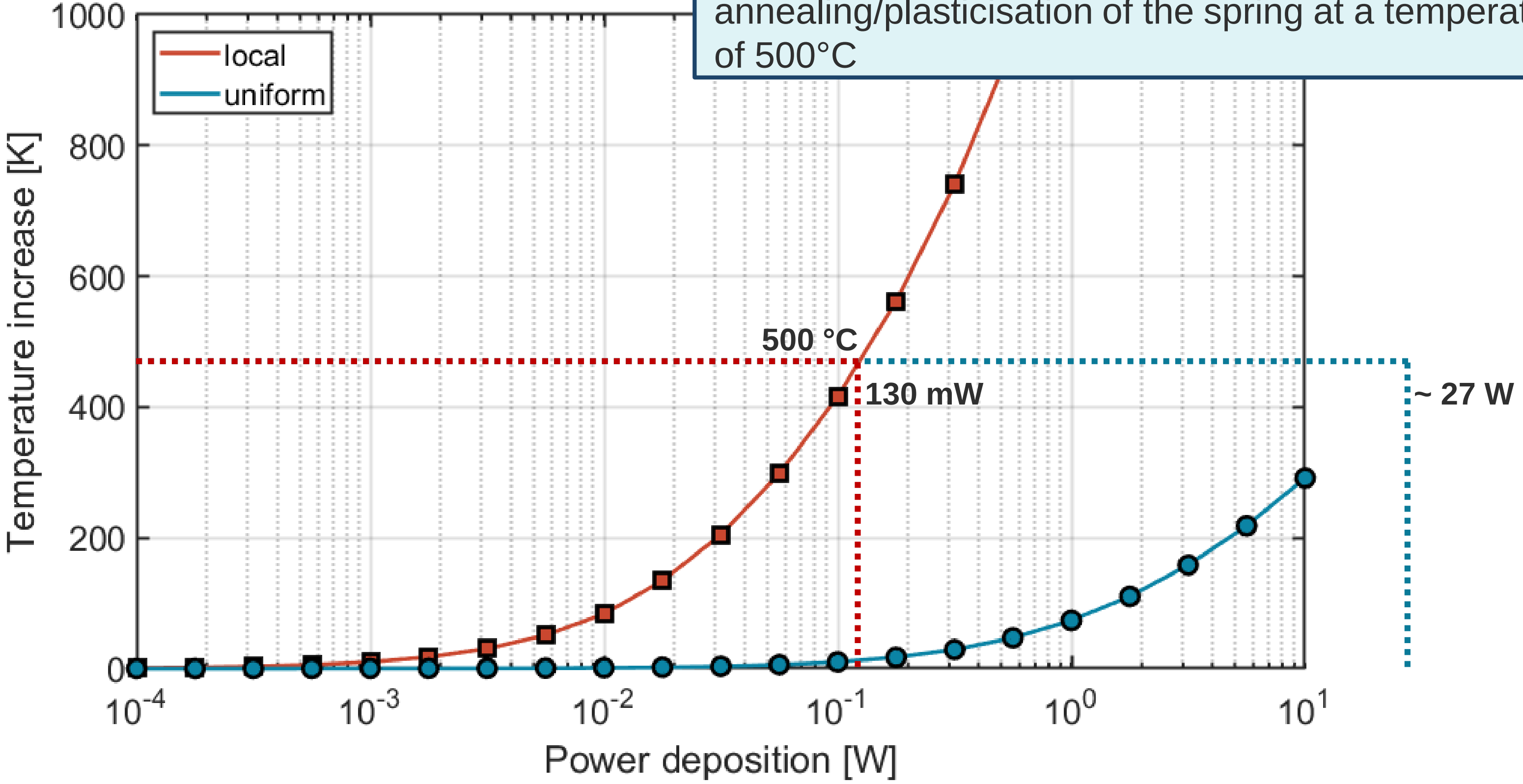

uniform

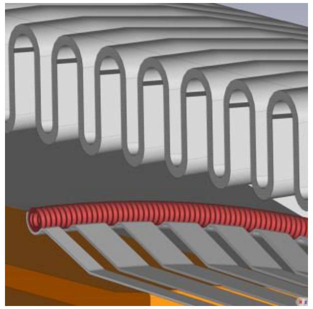

localised

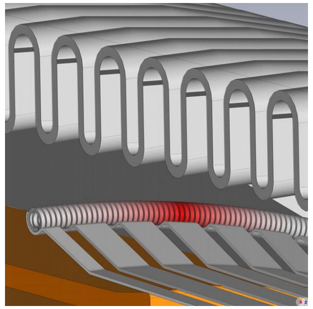

RF finger production

In 2004, BINP initiated the production using a single sheet of CuBe

- RF Finger width 3.6 mm
- Distance between fingers 1.47 mm

smaller spacing

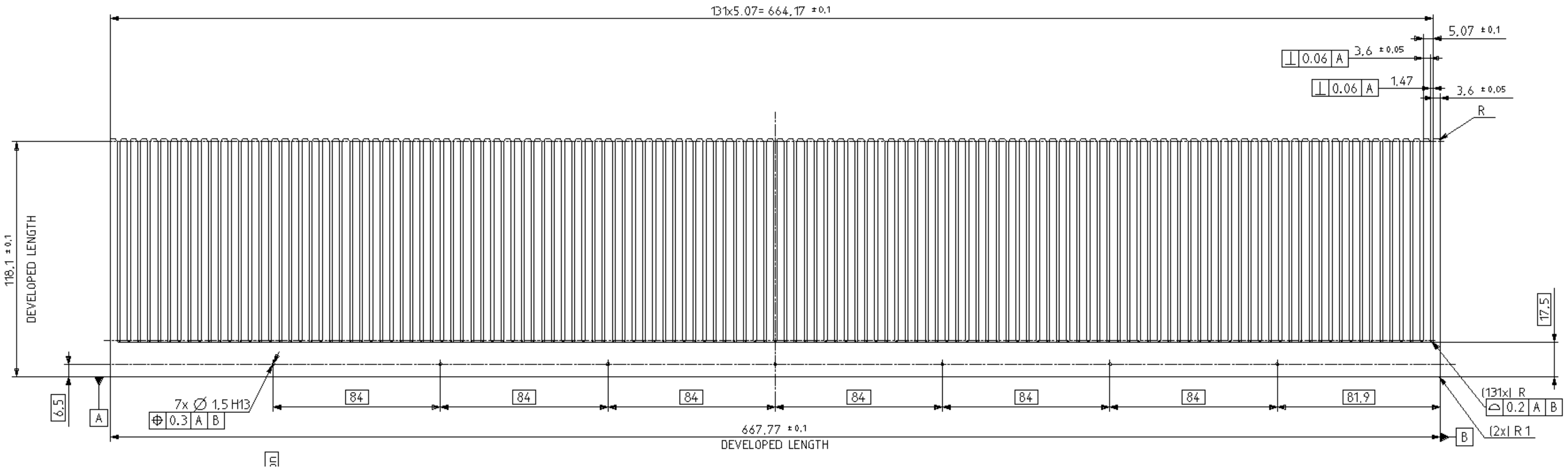

03

Impedance Assessment

Experiments and Simulations

Impedance measurements - field leakage

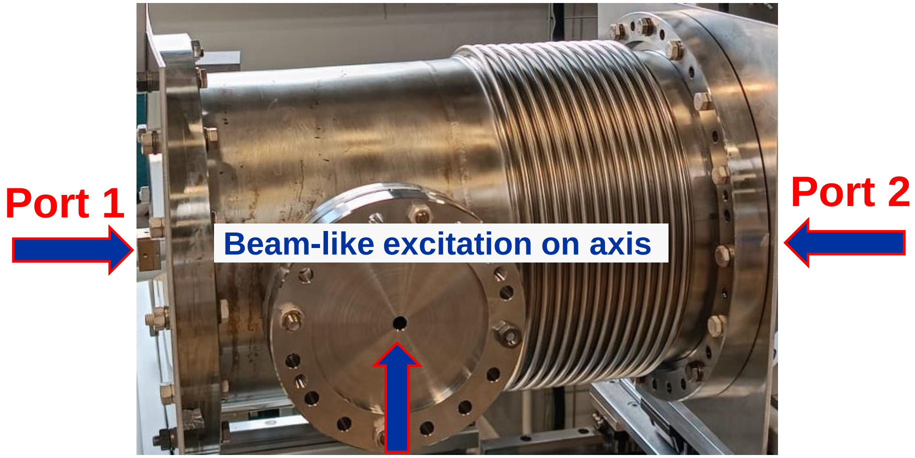

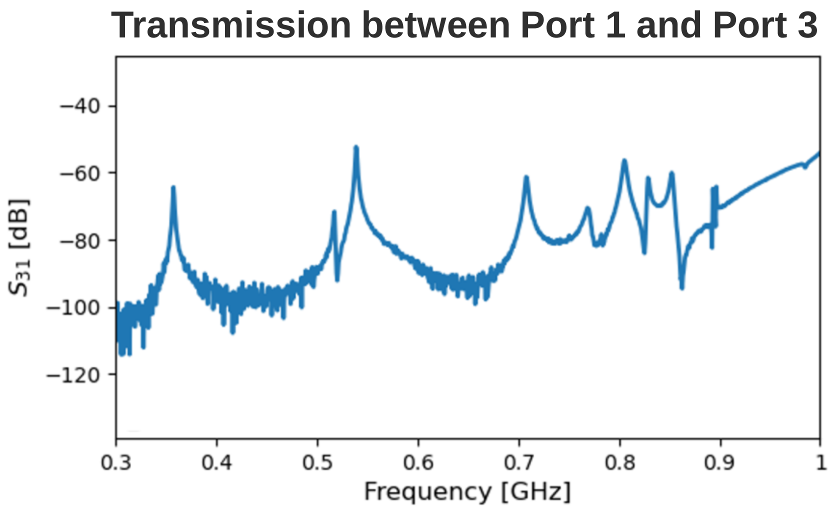

- Low frequency resonances (below vacuum pipe cut-off frequency)
  - **Field leakage** through RF fingers / transition tube

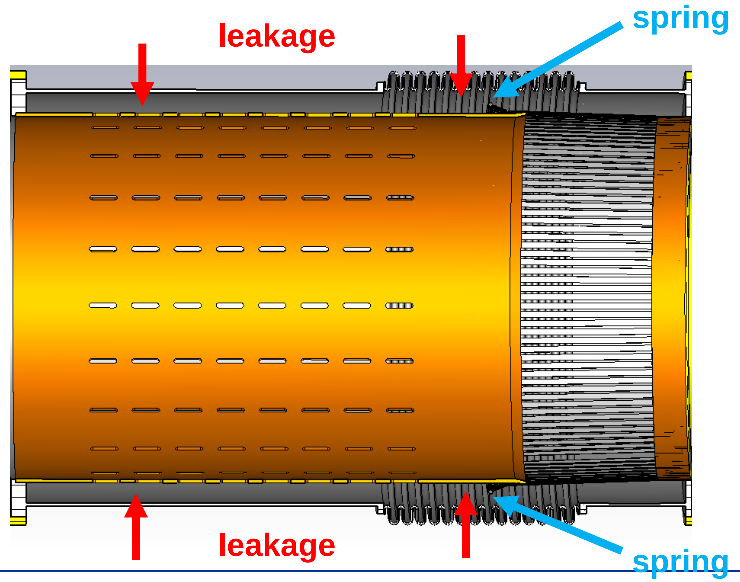

➢ **It is the mechanism that allows some of the beam induced power to be dissipated on the spring**

Electromagnetic simulation - field leakage

- The **simulations confirmed the presence of field leakage** from the fingers and the transition tube

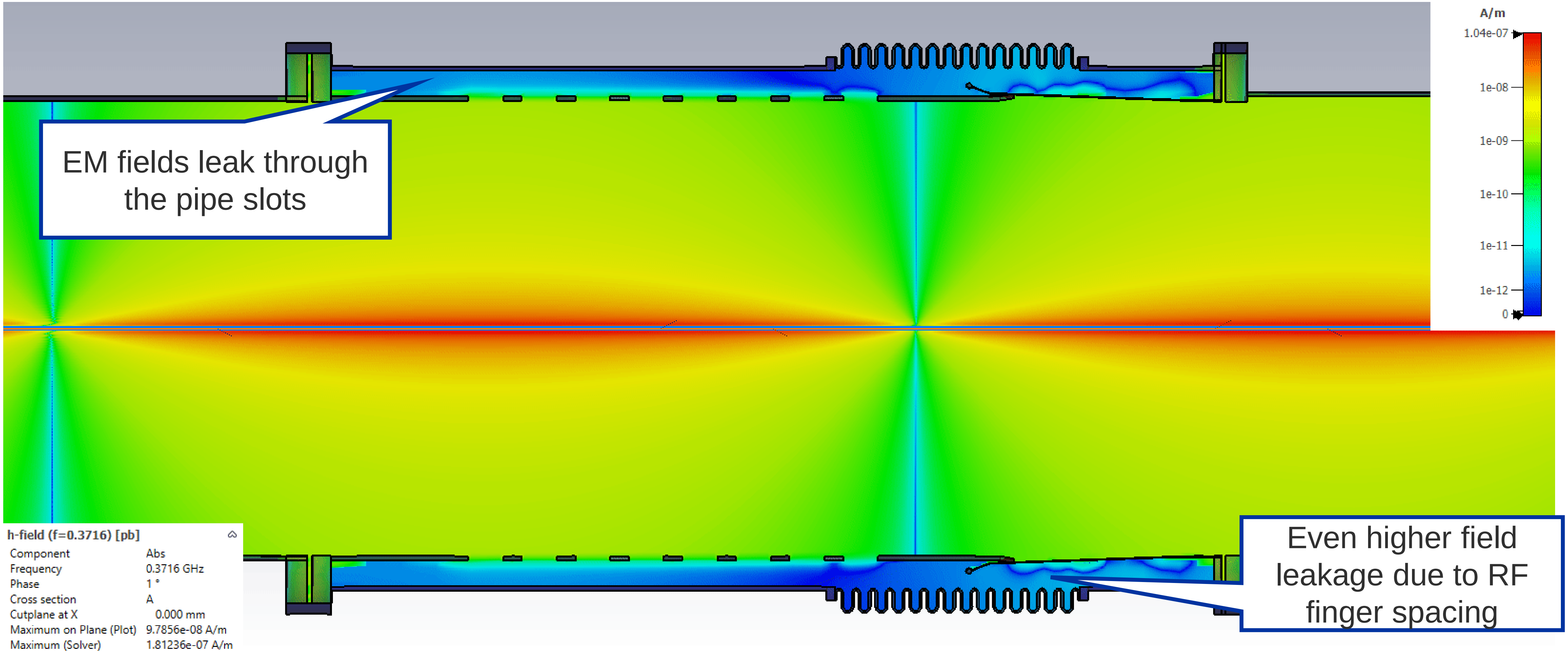

Simulations vs Measurements : validation of the model

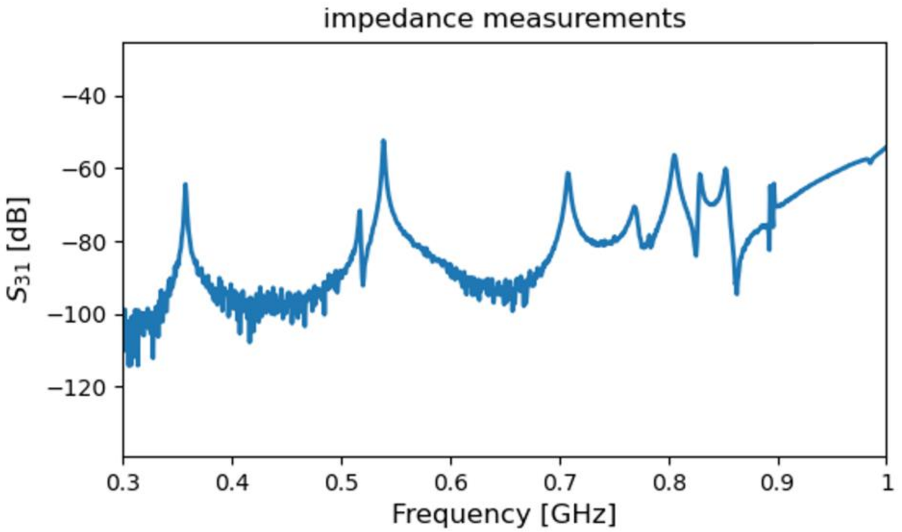

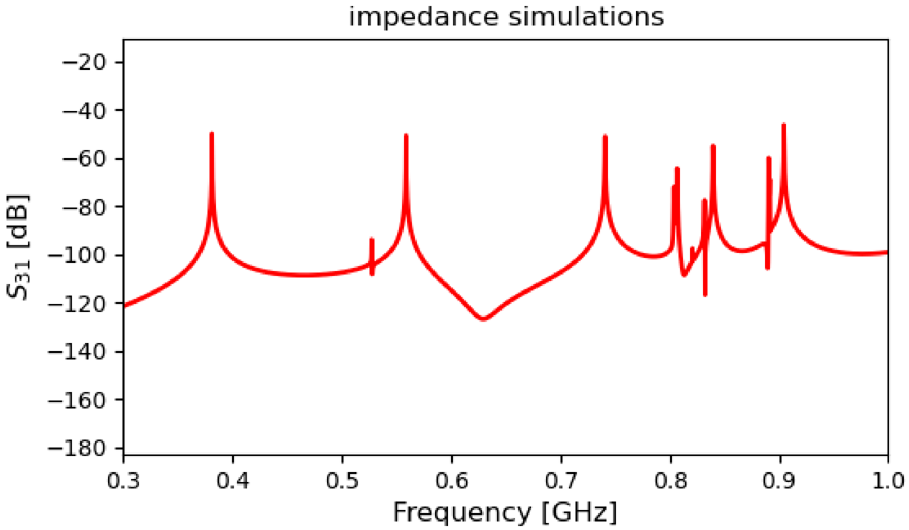

- Virtual measurement setup reproduced in e.m. simulation

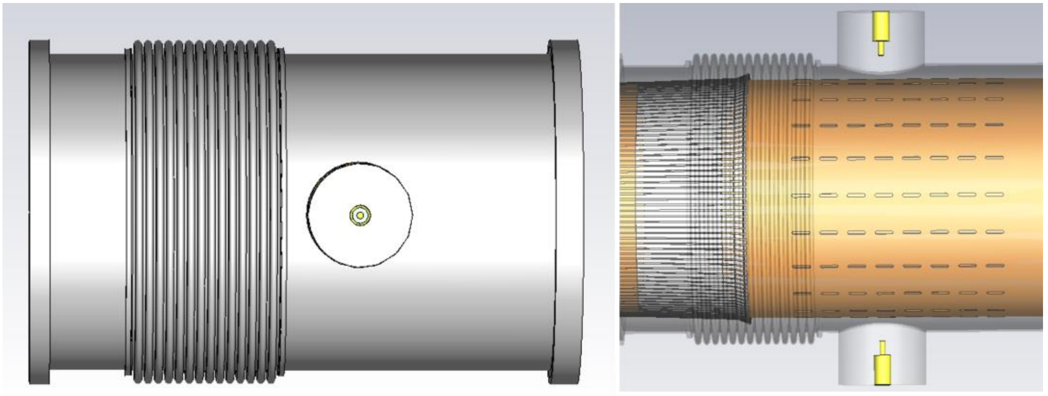

- Very **similar frequency response** between simulation and measurements
  - First resonance below 400 MHz
  - Several resonances below pipe cut-off frequency

The **simulation model is used for impedance assessment**

Beam induced power assessment

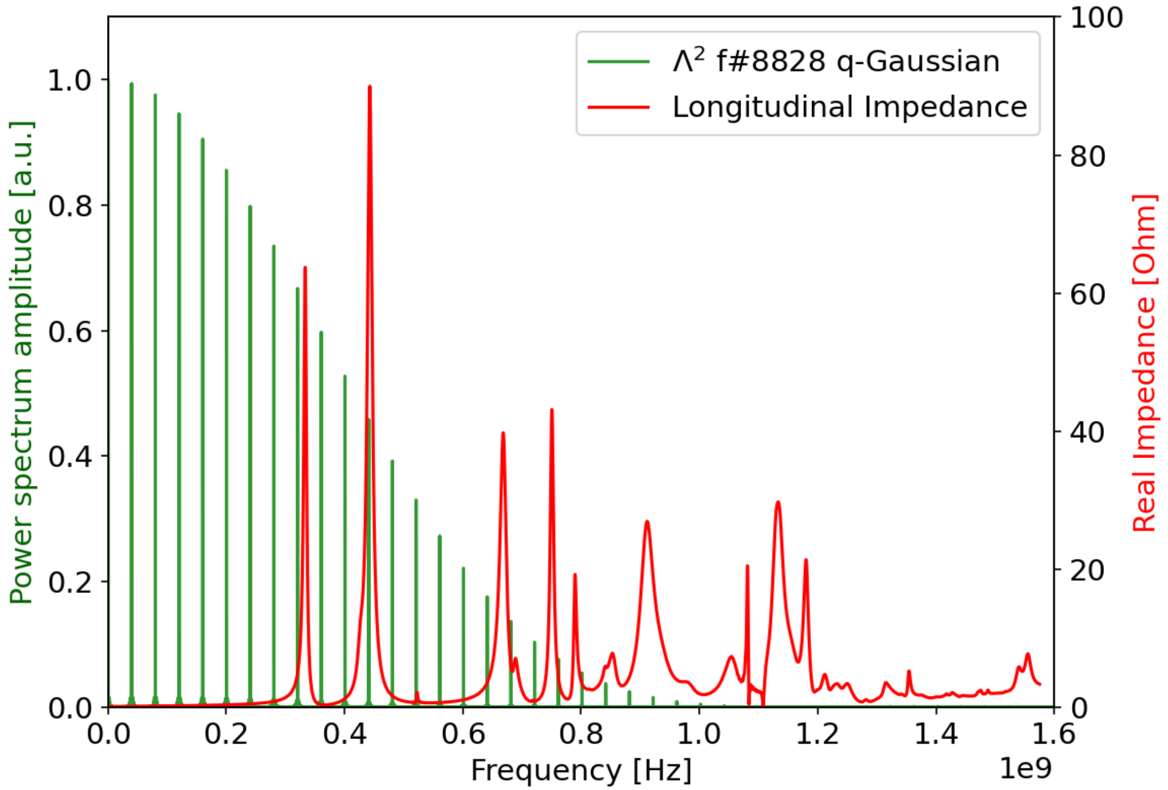

Λ: beam spectrum
ω_0: angular revolution frequency
Δy_1: offset of beam 1 from center
Δy_2: offset of beam 2 from center
$Z_{||}^{0,1}$: longitudinal impedances of orders 0 and 1
τ_s: delay between arrival times of the two beams

Two beam power loss

$$\Delta W(s) = \left(\frac{\omega_0}{\pi}\right)^2 \sum_{p=0}^{\infty} |\Lambda(p\omega_0)|^2 \{Re[Z_{||}^0(p\omega_0)] + [\Delta y_1(s) + \Delta y_2(s)]Re[Z_{||}^1(p\omega_0)]\}(1 - cos p\omega_0\tau_s)$$

*** Power loss calculation in separated and common beam chambers of the LHC, C. Zannini, G. Rumolo, G. Iadarola, 5th International Particle Accelerator Conference, Dresden, Germany, June 2014**

Different scenarios studied

Design case
- Symmetric RF fingers distribution
- Perfect contact fingers-transition tube

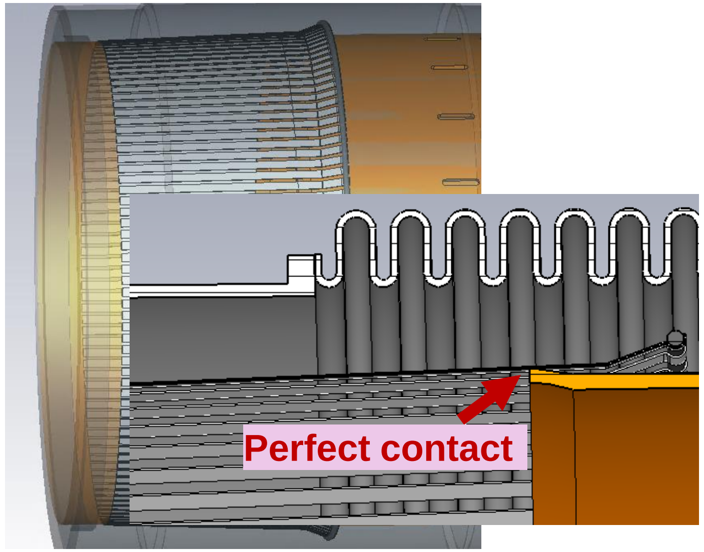

Ideal contact case
- Non symmetric RF fingers distribution
- Perfect contact fingers-transition tube

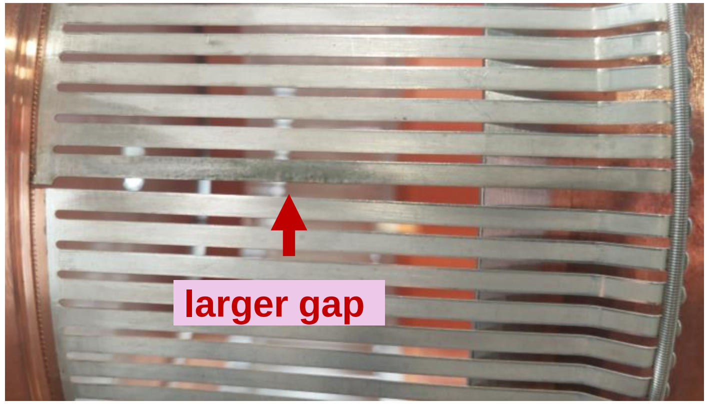

Degraded contact case
- Non symmetric RF fingers distribution
- Degraded contact fingers-transition tube

Lost contact case
- Non symmetric RF fingers distribution
- **Lost contact fingers-transition tube**

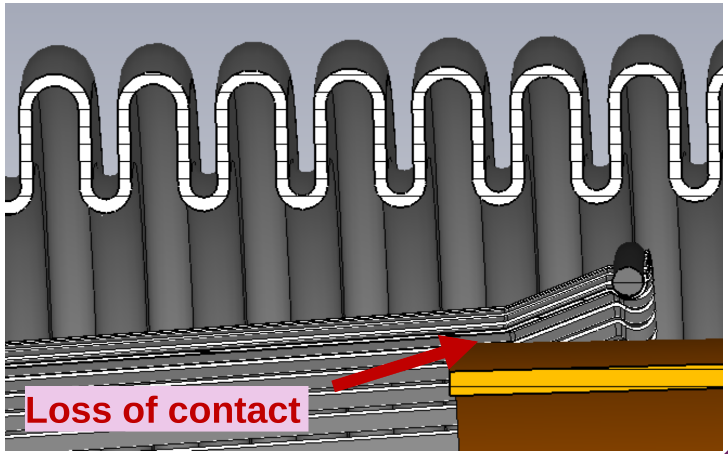

- **Impedance is more affected by production defects especially in presence of beam offset**

- **Contact degradation between fingers-transition tube largely increases the beam induced power on the spring**

Beam induced power loss on the spring

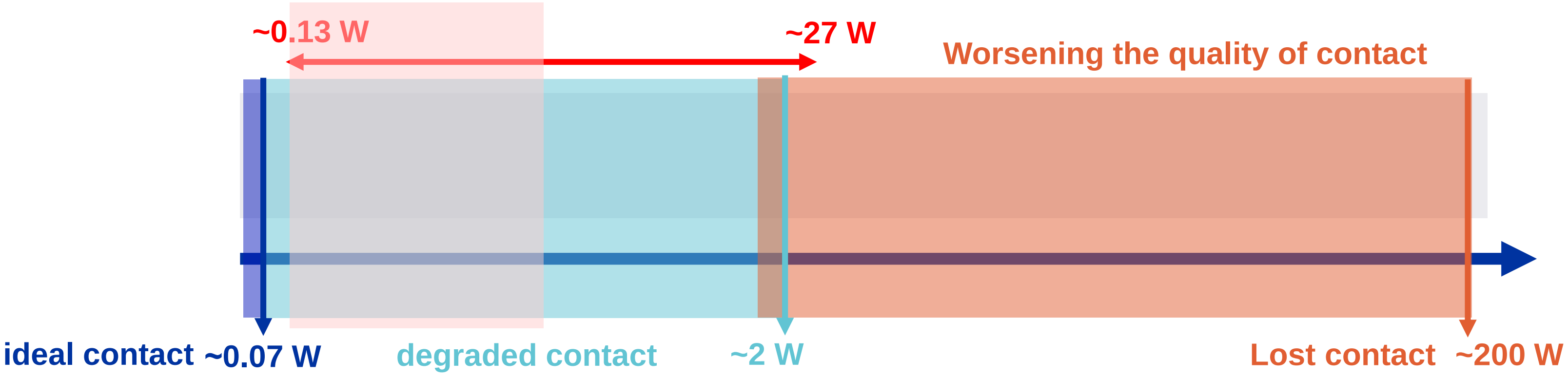

Annealing condition

- Temperature above 500° C
- ~0.13 W for localized power
- ~27 W for distributed power

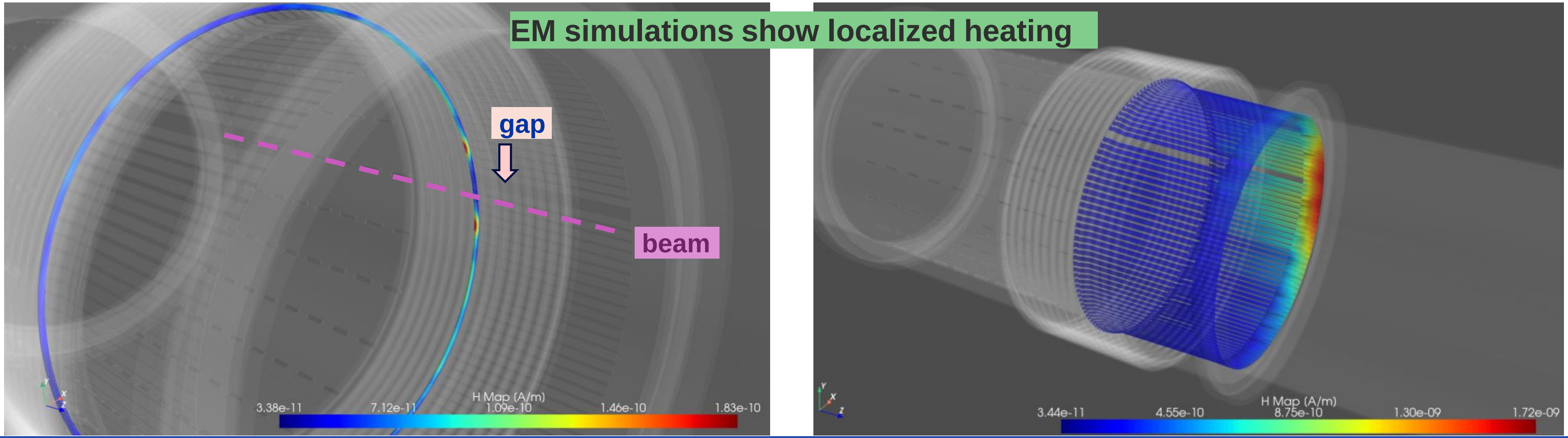

IP4, IP8: observed finger degradation

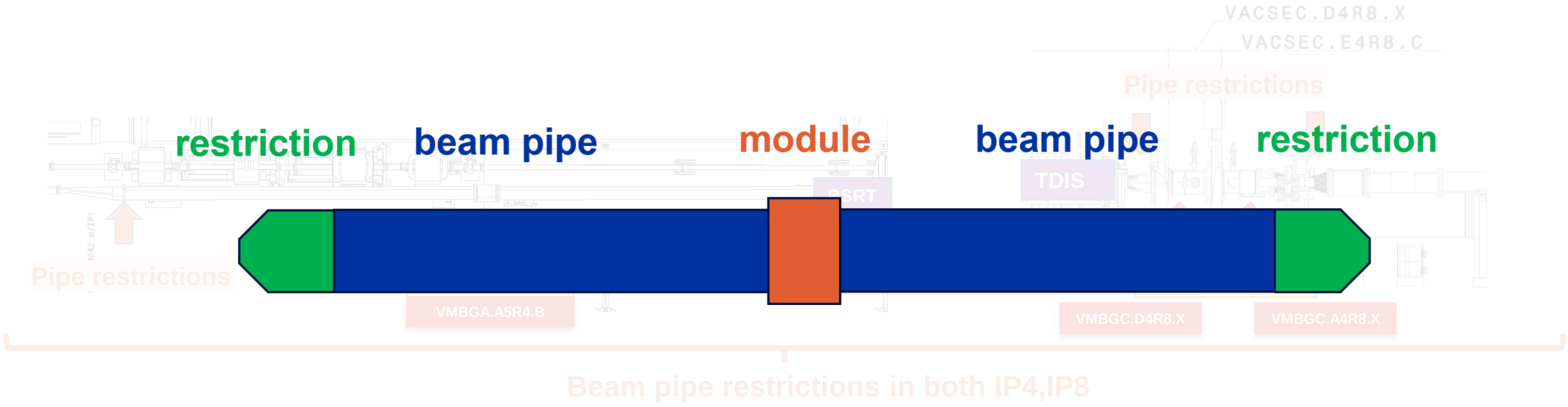

- **In IP4,IP8 the degradation mechanism is somewhat different**
  - Due to the restriction of the beam pipe → cavity-like structures
    - Forest of quite strong resonances
      - power could be dissipated on the fingers
      - From thermal studies : it could explain fingers degradation

Disclaimer : preliminary results

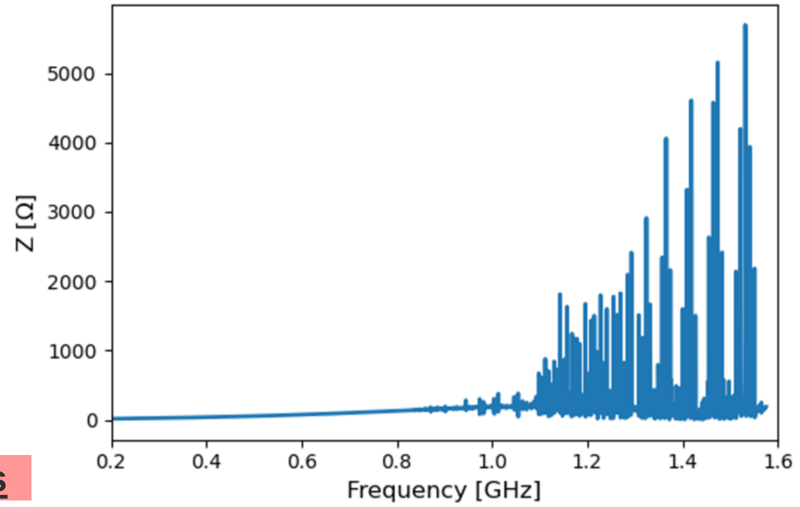

04

Possible Mitigation Strategies

Ongoing Impedance and Vacuum Studies

Essence of the mitigation strategy

Replace and transform the current 71 modules in the ID212.7 RF contact **with newly designed modules** wherever it is possible to implement such a substitution .
Anchor ‘unnecessary’ ID212.7 modules **(EDMS)**

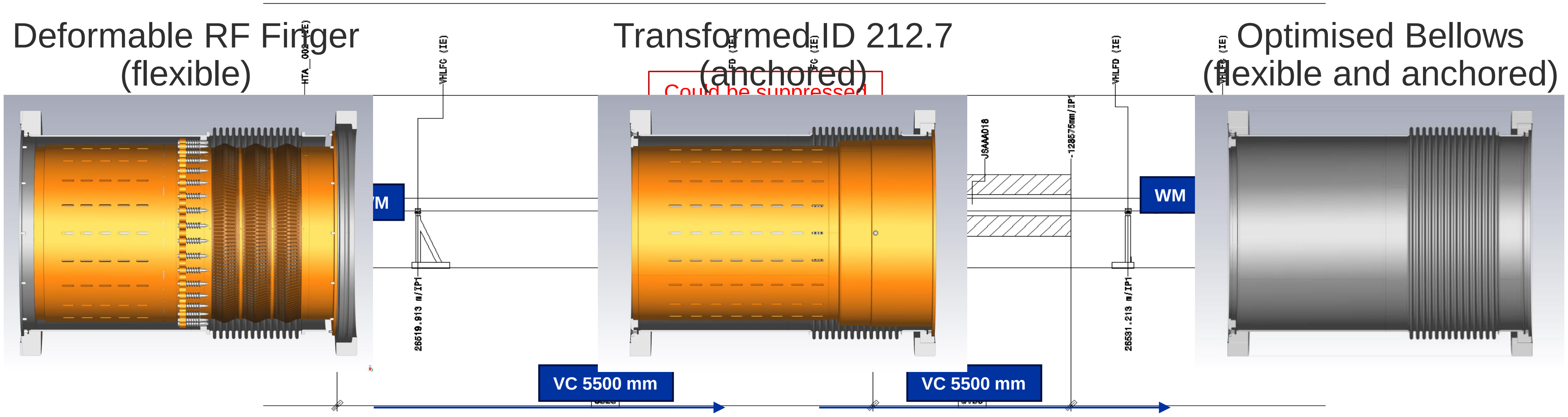

Deformable RF Fingers – DRF

No spring and no possibility to lose electric contact

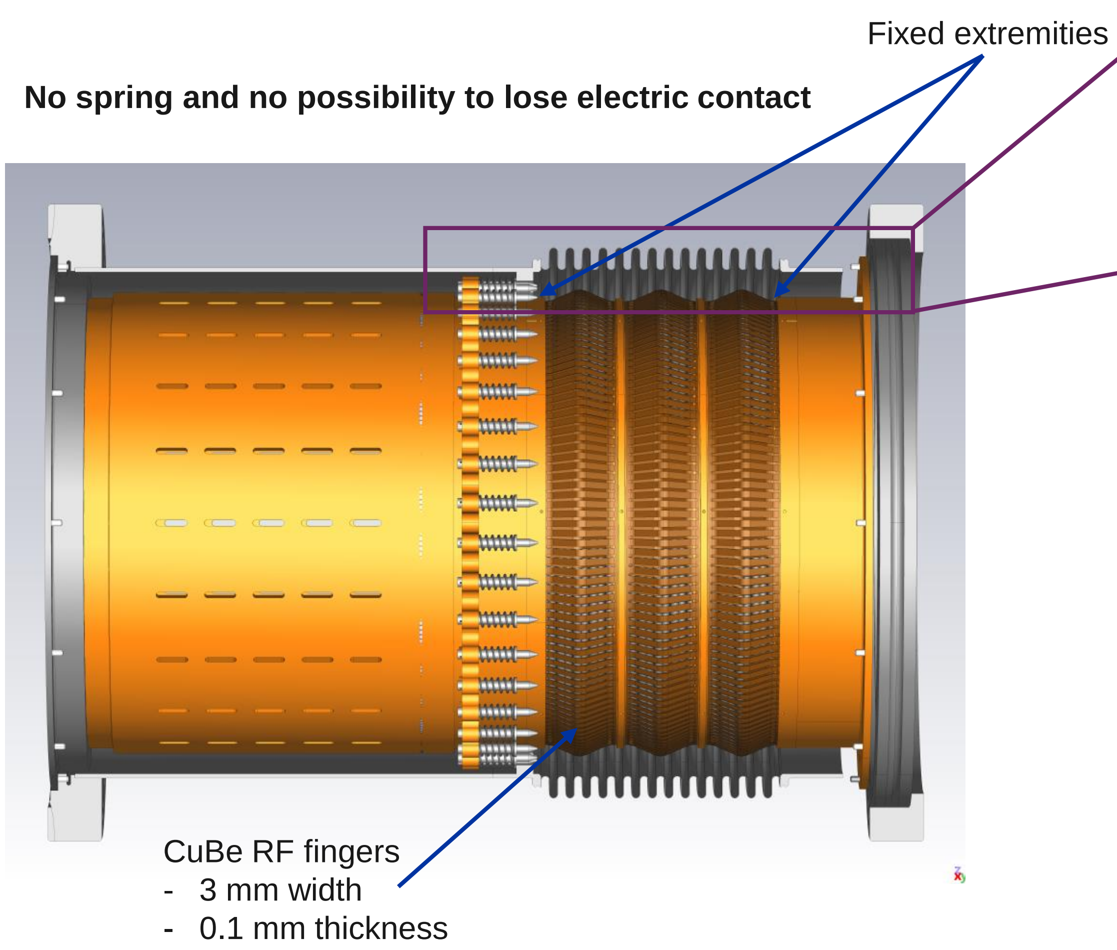

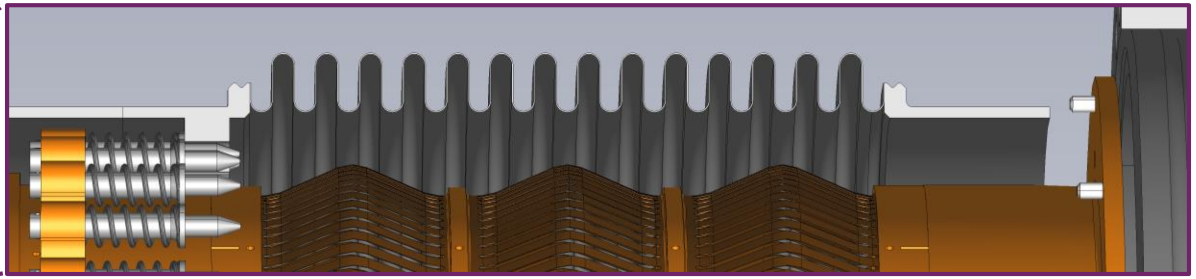

A Nominal height of 2.7 mm (**11° angle**) is considered for the **nominal operation position**.

Evaluation of the cumulative impact of 25 Modules on the LHC:

- The additional impedance contribution is compatible with beam stability requirements **(EDMS)**

Transformed ID212.7 Module in straight vacuum chamber

Fixed Positioning

- Reallocate the thermal expansion during bake-out cycles to designated bellows

Robust thermal endurance

- 10 mm solid copper material, engineered to withstand substantial heat loads should they manifest

Impedance

- Expected to behave as a straight vacuum chamber

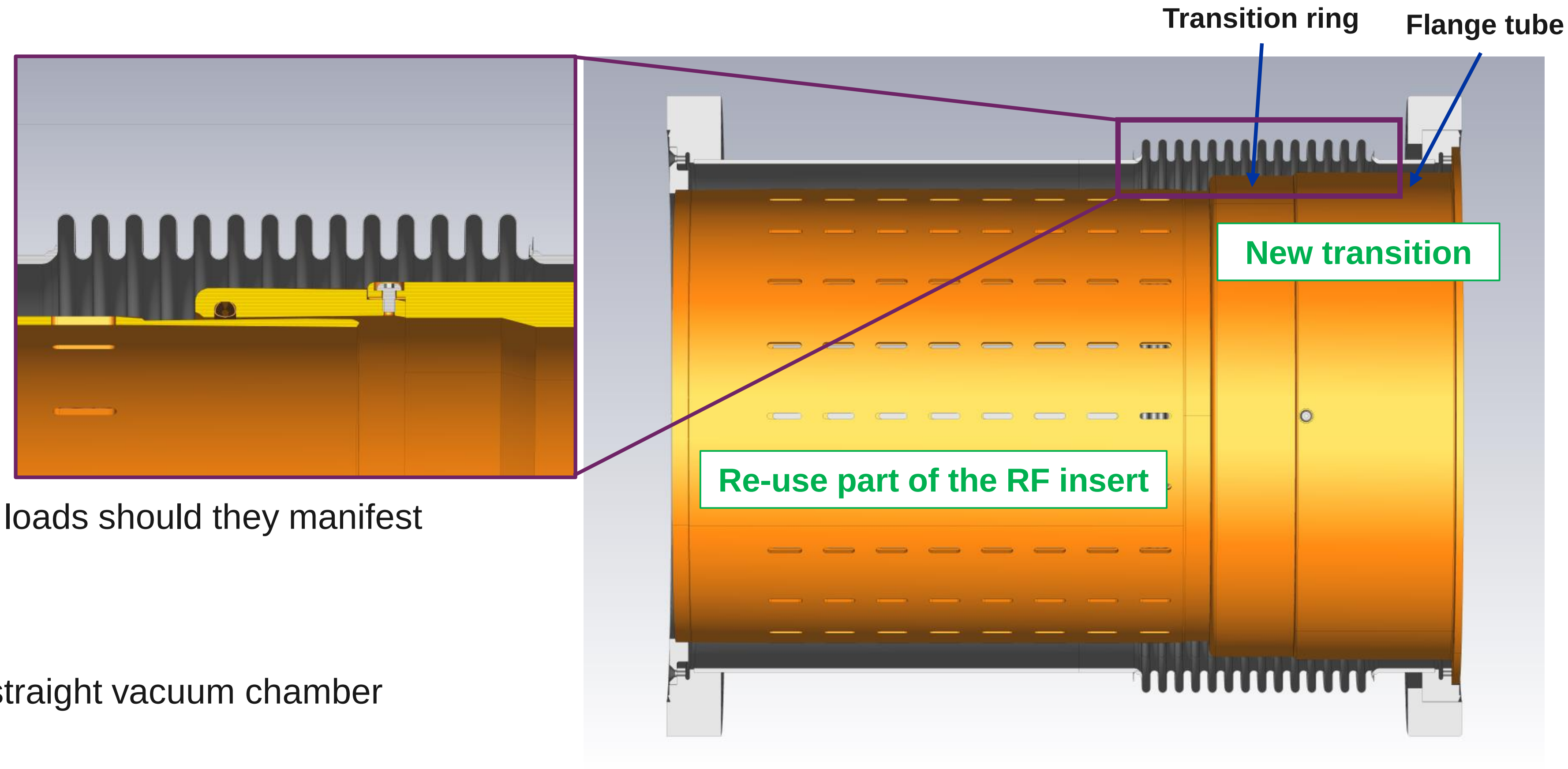

Optimised Bellows

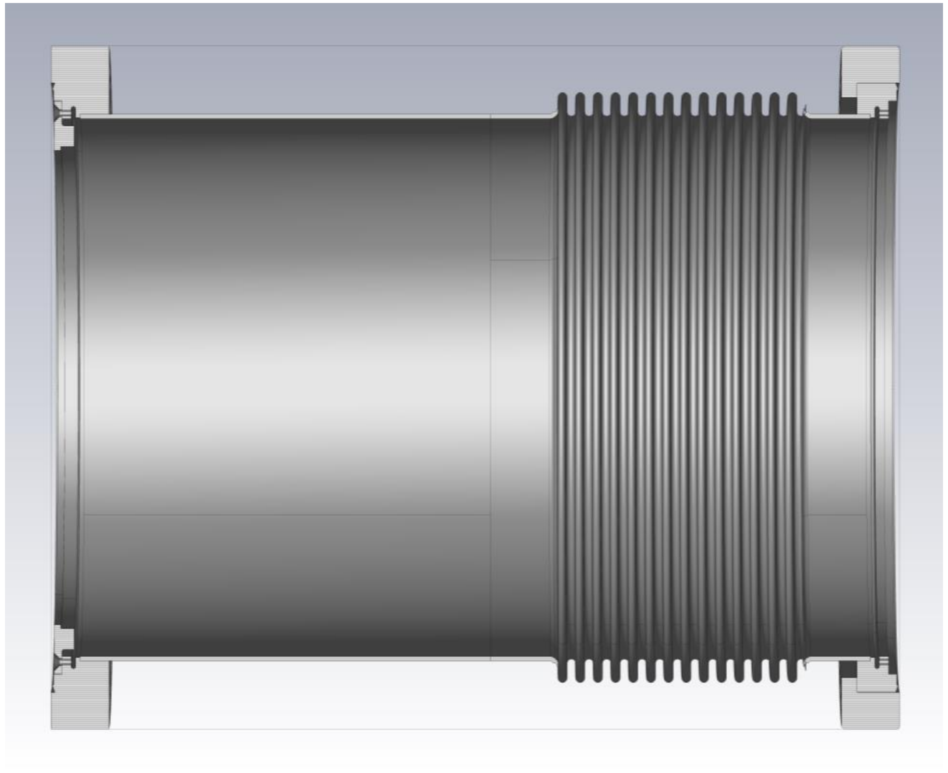

13 Convolutions Bellow Ø 212.7 mm Stainless Steel

Secure choice concerning mechanical and thermal considerations

Rapid and cost-effective production

Higher impedance compared to the ID212.7 RF contact fingers

- Longitudinal and transverse impedance will be affected
  - to be studied in detail

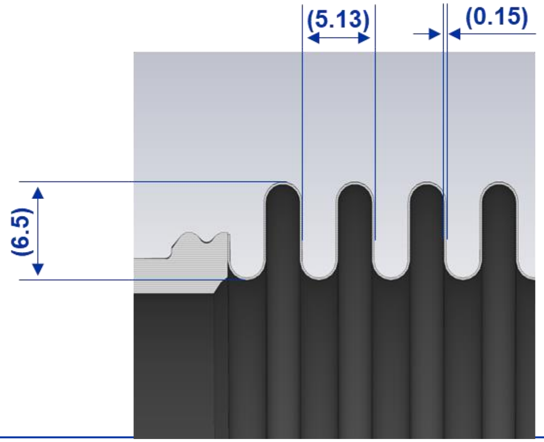

Essence of the mitigation strategy

Replace and transform the current 71 modules in the ID212.7 RF contact **with newly designed modules** wherever it is possible to implement such a substitution.
Anchor ‘unnecessary’ ID212.7 modules (EDMS)

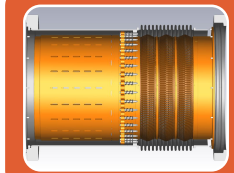
Deformable RF Fingers

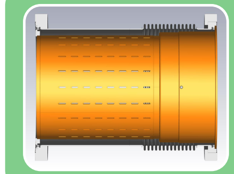
Transformed ID 212.7 Modules

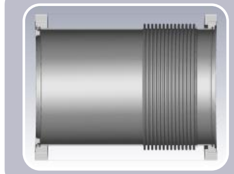
Optimised Bellows

Two-stages approach

- Total — **Modules 71**
- EYETS 23/24 — **Replaced modules 47**
- YETS 24/25 — **Replaced modules 24**

Full consolidation in YETS 24/25

Conclusion and Outlook

Do we expect additional failure in 2024 run?

- **1 Failure** observed **only** in 2023 with a maximum total intensity of ~3.8e14 p. (with 1.63e11 ppb)

  - **Localized heating on spring enhanced by the beam offset and production defects**

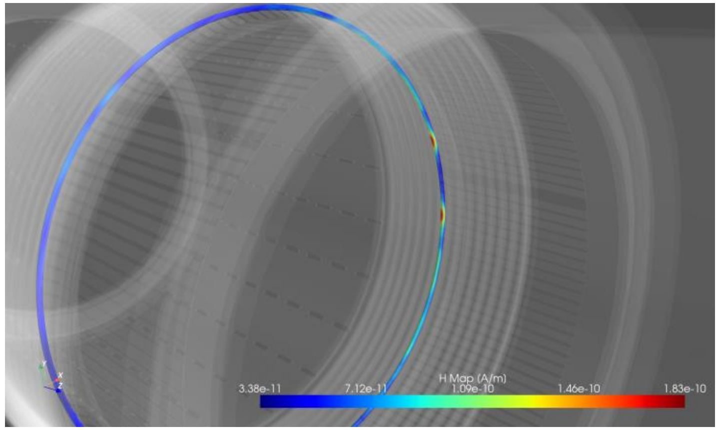

  - **24 module will keep the original spring+finger design**
    - **No failure** expected with **ideal contact**
    - Failure can occur due to degraded contact quality
      - **An intensity threshold cannot be identified due to the strong dependence on contact quality**

  - **Other possible failure mechanism** (preliminary results)
    - Damage of RF fingers in IP4,8
      - heating of the RF fingers due to the machine layout

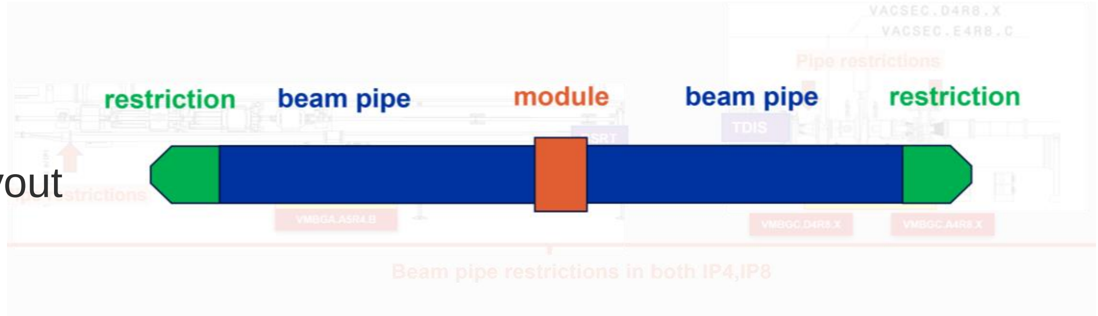

BE-ABP
Chiara Antuono
Elena De La Fuente
Riccardo De Maria
Stéphane Fartoukh
Lorenzo Giacomel
Nicolas Mounet
Yannis Papaphilippou
Giovanni Rumolo
Benoit Salvant
Leonardo Sito
Carlo Zannini

EN-MME
Thibaut Coiffet
Alessandro Dallocchio
Florent Fesquet
Ana Teresa P. Fontenla
Damien Jerome Foresy
Gonzalo A. Izquierdo
Jean-Marc Malzacker
Alexandre Porret
Laurent Prever-Loiri

On behalf of…

SY-RF
Ivan Karpov
Christine Vollinger

home.cern

TE-VSC
Giuseppe Bregliozzi
Sergio Calatroni
Paolo Chiggiato
Isabel Cuevaz
Thomas Da Silva
Florent Fesquet
Alessio Galloro
Jan Hansen
Patrick Krkotic
Fabrice Santangelo
Orlando Santos
Josef Sestak
Benoit Teissandier
Marc Thiebert

TE-MSC
Mariano Pentella

Thank you for your attention!

Any questions?

home.cern

Backup

Simulations Vs measurements : validation of the model

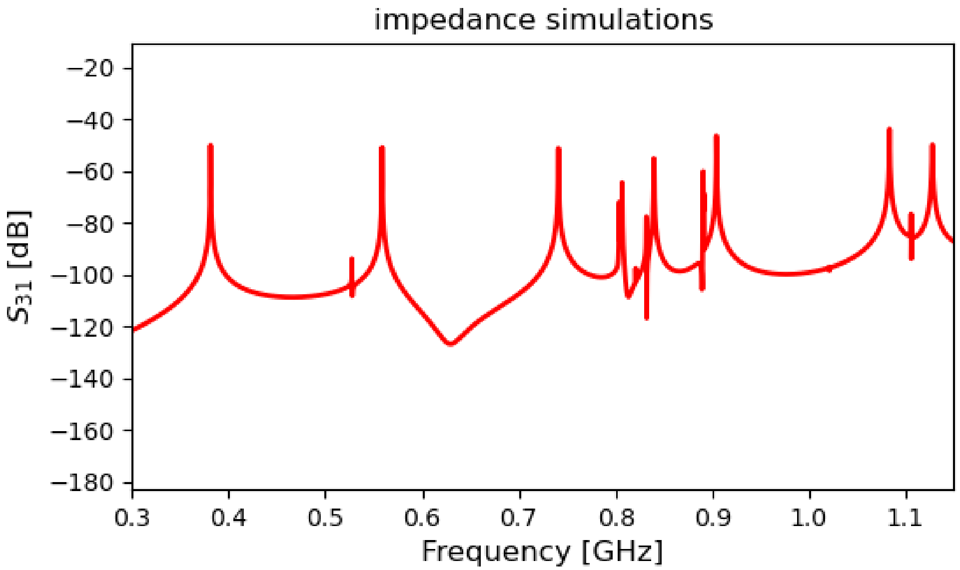

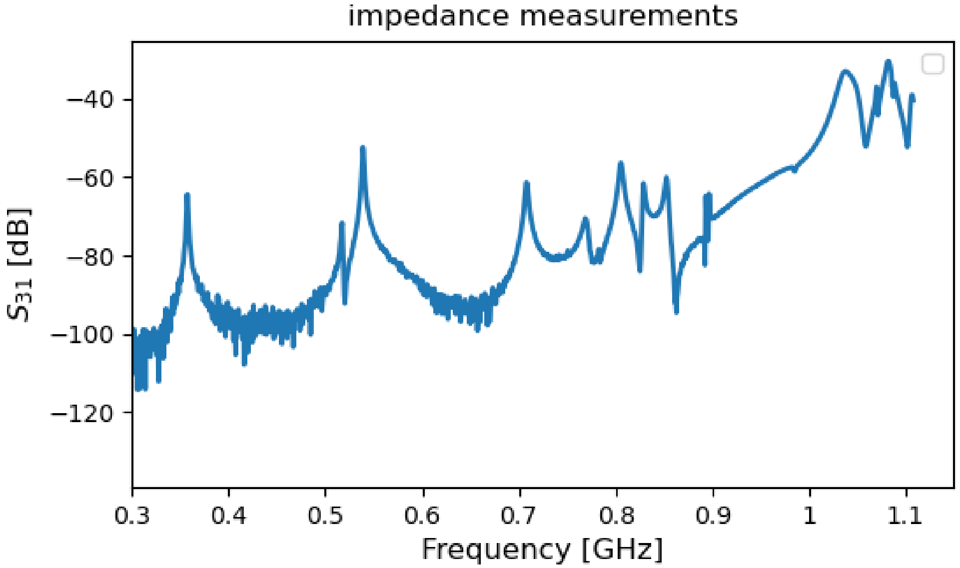

Do we expect failure of the smaller modules?

Smaller diameter modules are expected to be less critical

- higher frequency modes
- Only 1 beam
- smaller beam offset
- less production defects
- lower impact of the machine layout

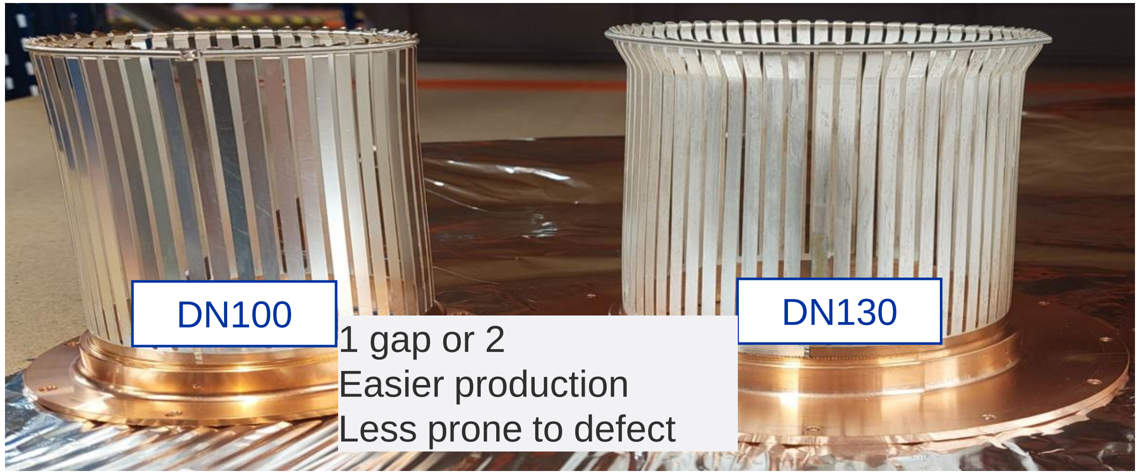

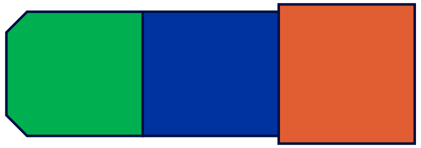

Smaller transition in terms of diameter

From G. Bregliozzi, LMC

- How many modules built from 3 segments do we have in the LHC machine?
  - ID212.7 & ID196 -> 71 units in total
  - DN130 & DN100 have 2 segments: Less prone to gap problems (Max aperture <2-3 mm)
  - DN80 & DN63 one single segments: Respected the tolerances of the drawings.
- Can this problem happen to the other RF inserts?
  - If the problem with the increased spacing is confirmed there is no reason to have the same failure module with warm modules inserts DN80 and DN63. DN130 and DN100 need further studies.

Spring Properties

Stainless Steel 1.4310 – AISI 301 (X10CrNi18-8)

- Good mechanical properties and corrosion resistance
- Capable of high tensile strength following cold work
- Tensile strength: 2239-2254 N/mm²

- Magnetic following cold work

Spring of module 5

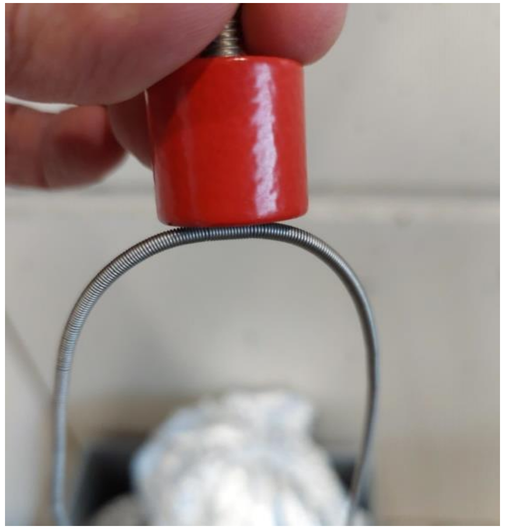

…but most of it is totally amagnetic

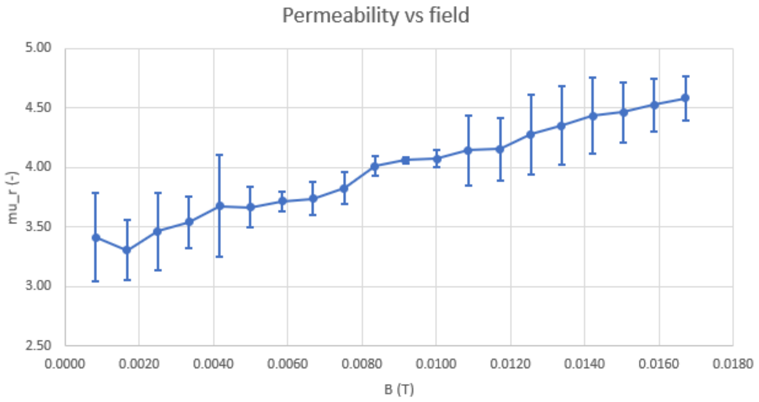

The material 1.4310 can theoretically be used up to +250°C.
After production, the spring is heat treated. At least 30min at 250°. Then cool at room temperature.

X rays – A4L1

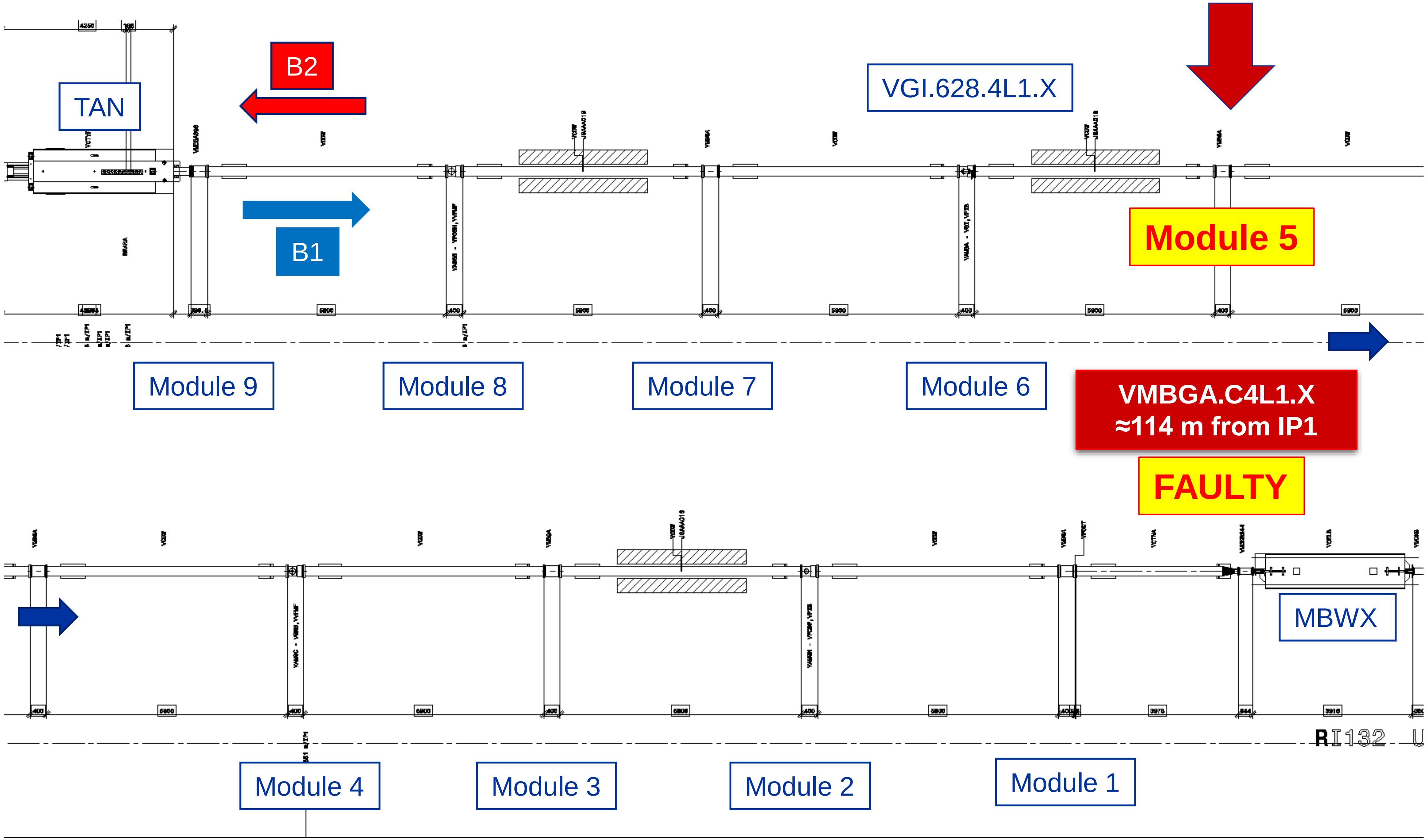

TAN
B2
B1
VGI.628.4L1.X
Module 5
Module 9
Module 8
Module 7
Module 6
VMBGA.C4L1.X
≈114 m from IP1
FAULTY
MBWX
Module 4
Module 3
Module 2
Module 1

X Rays – VMBGA.B4R5.X – Module 3

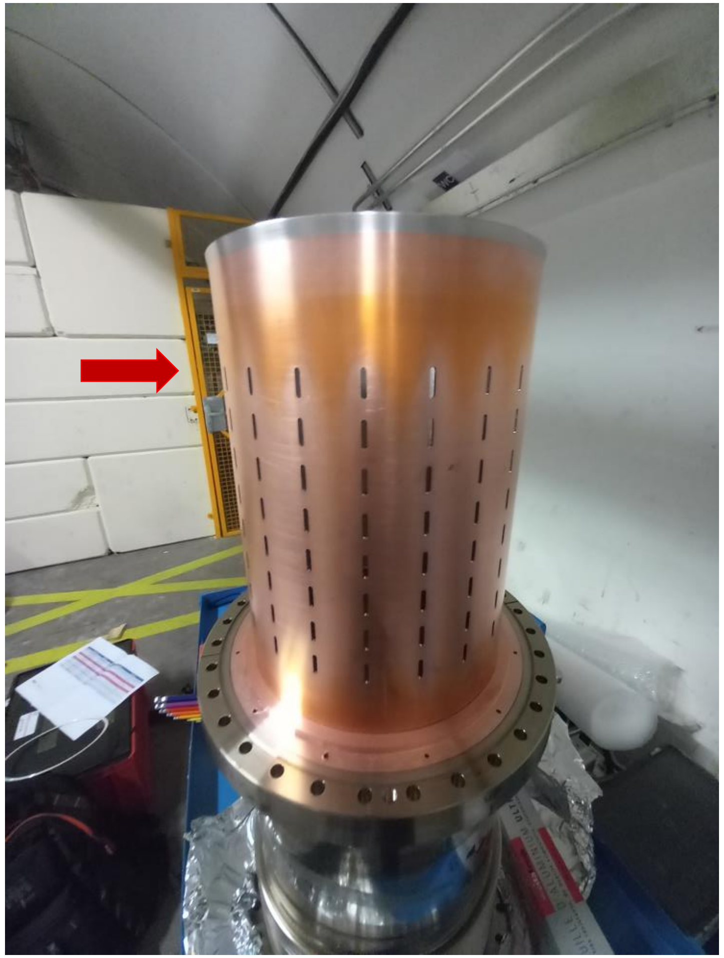

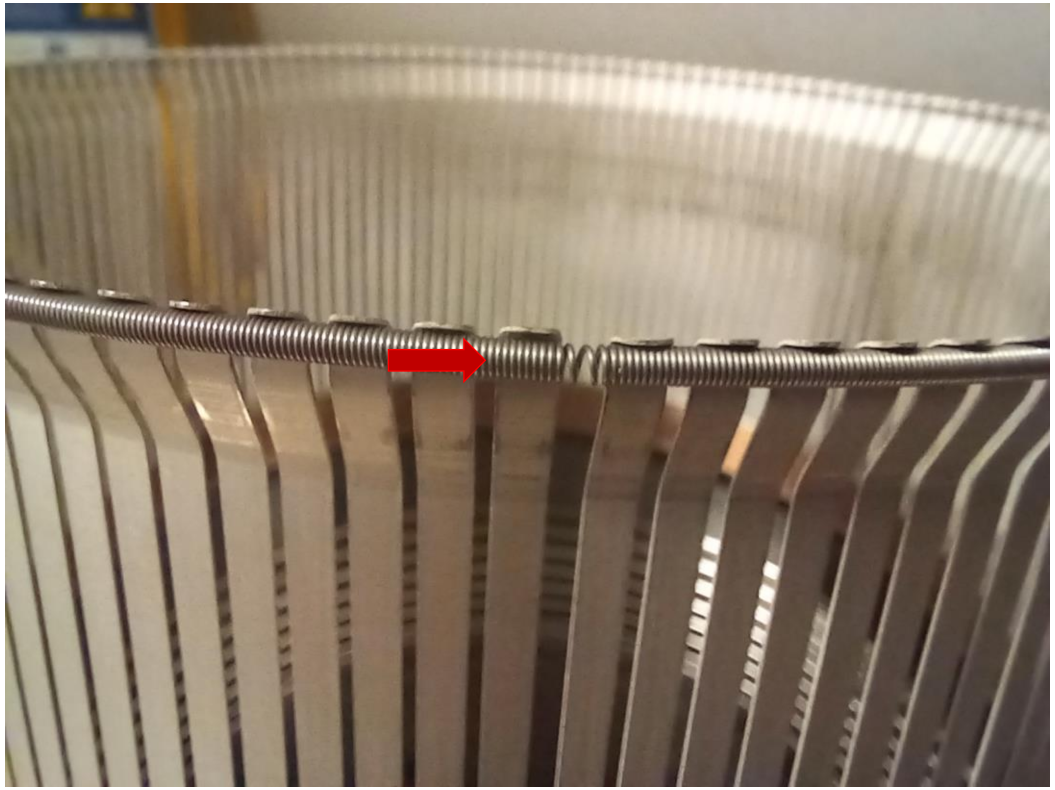

X rays – A4L8
Double Beams

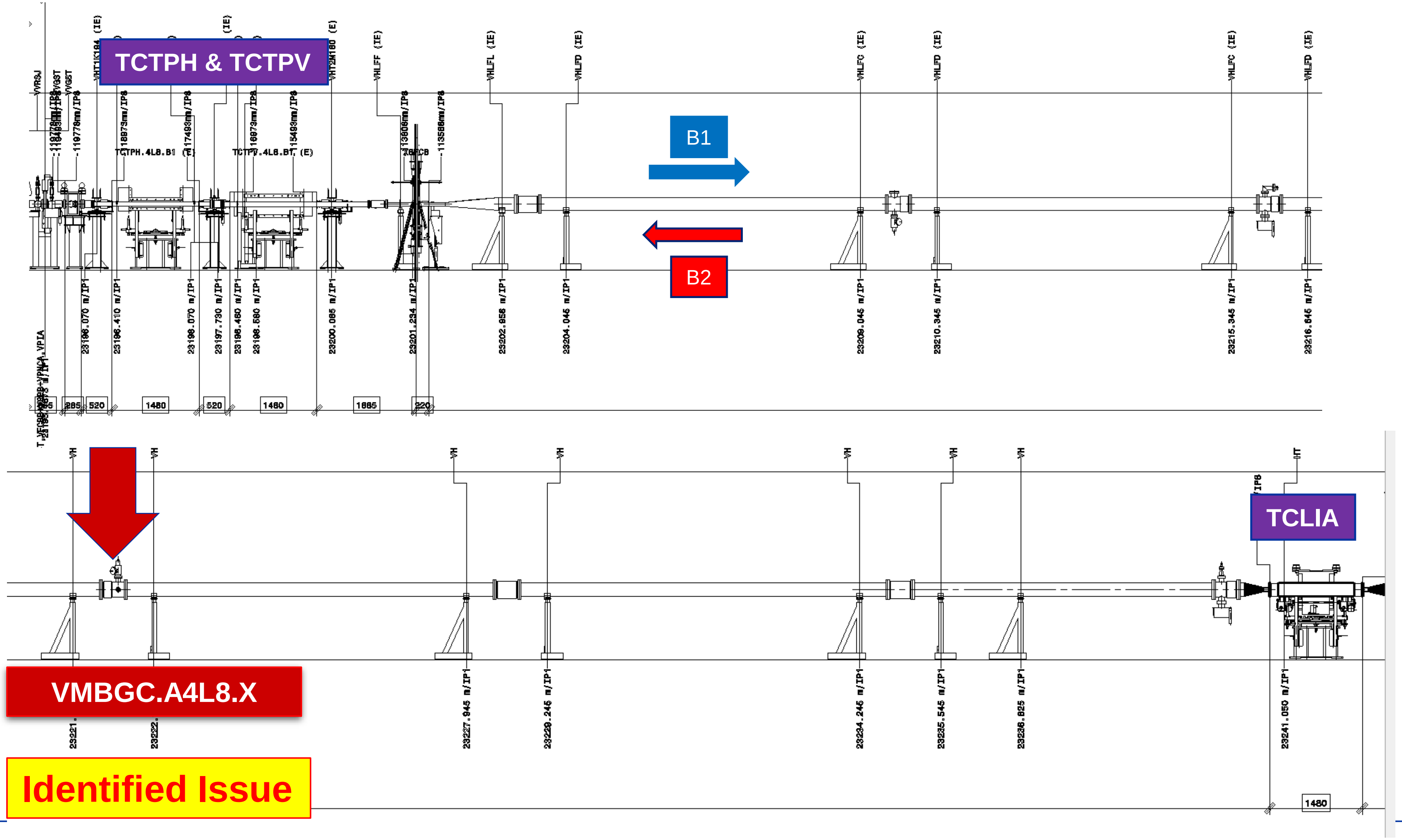

X rays – A4R8 (E4R8.X8)
Double Beams

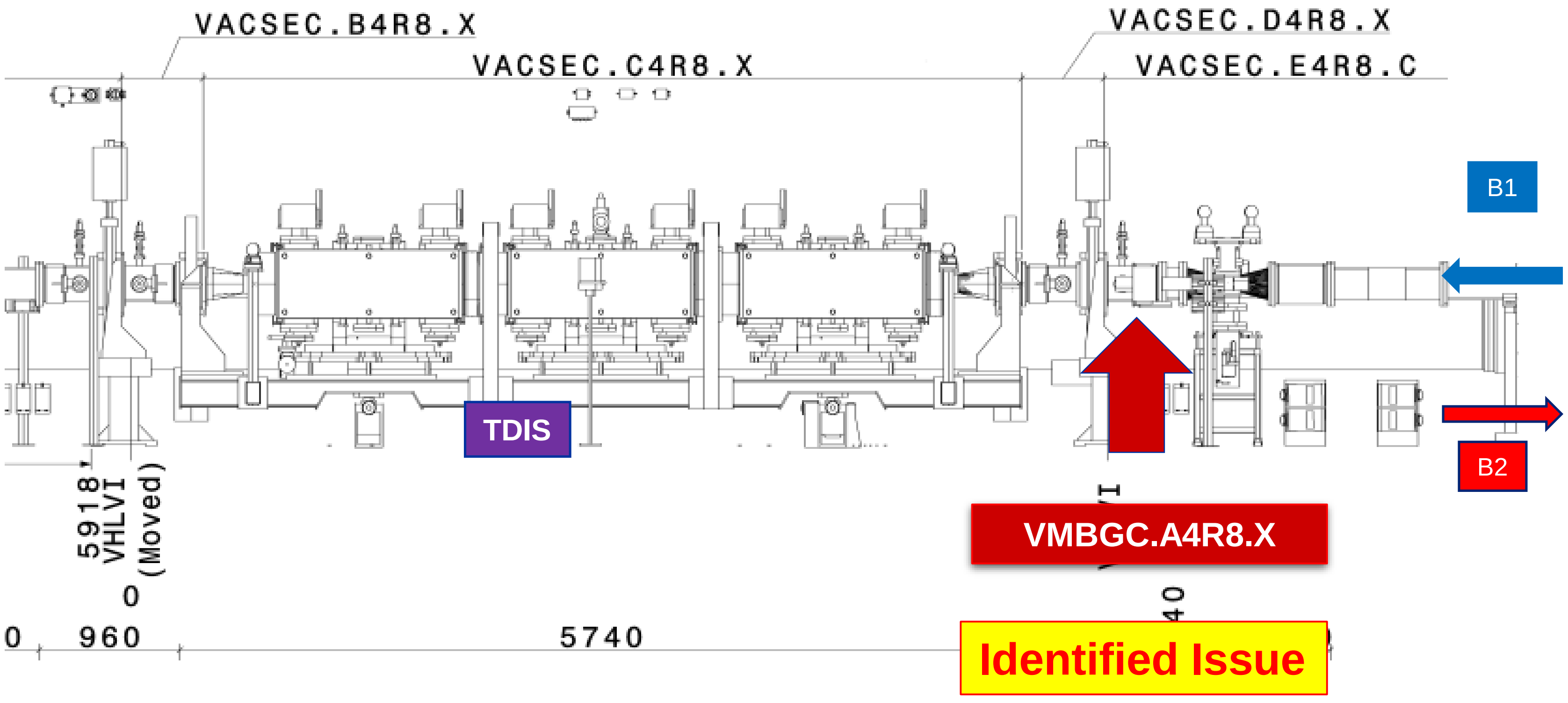

B4R8.X - VMBGC.E5R8.X

No spring coil degradation detected

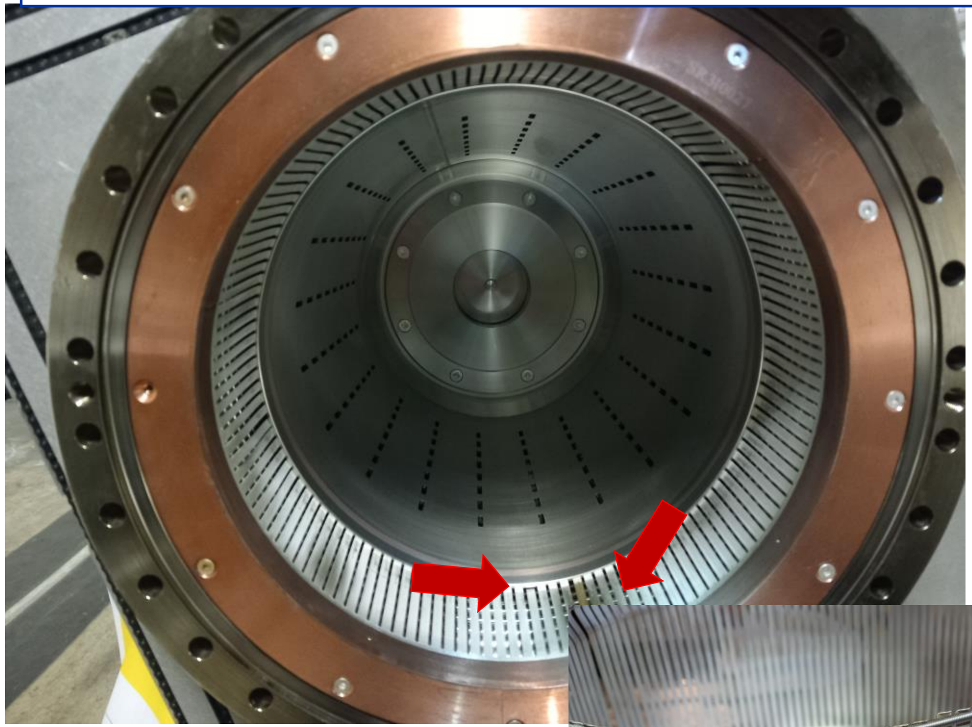

X rays – D5R4
Single Beam

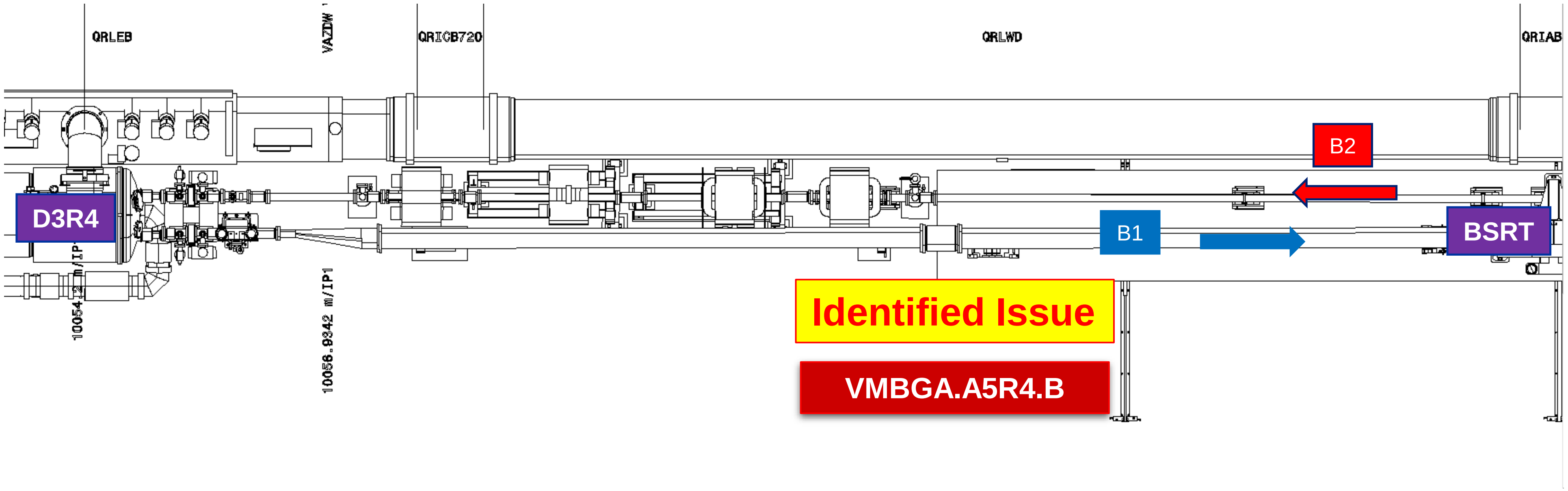

Pictures of VMBGA.A5R4.B

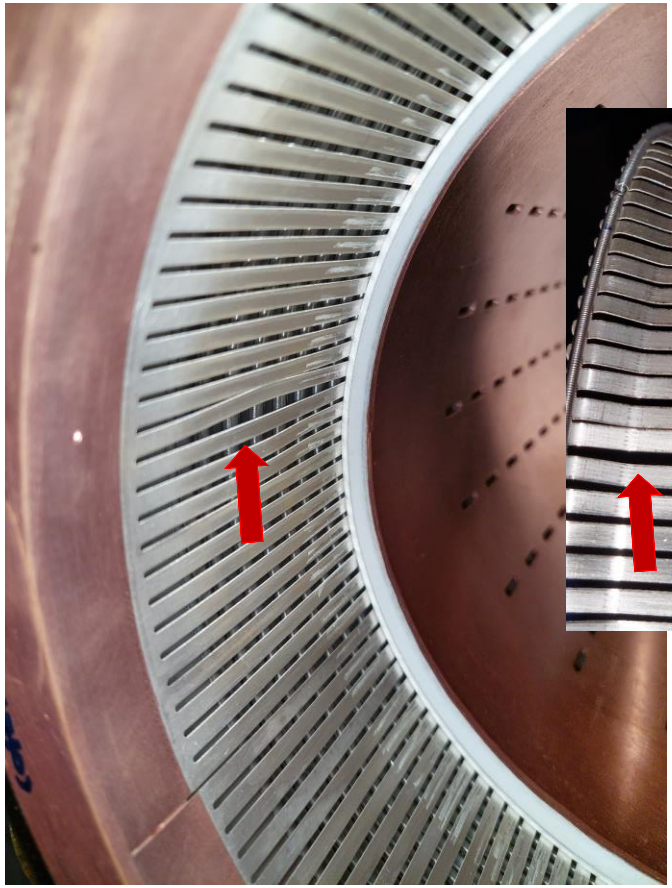

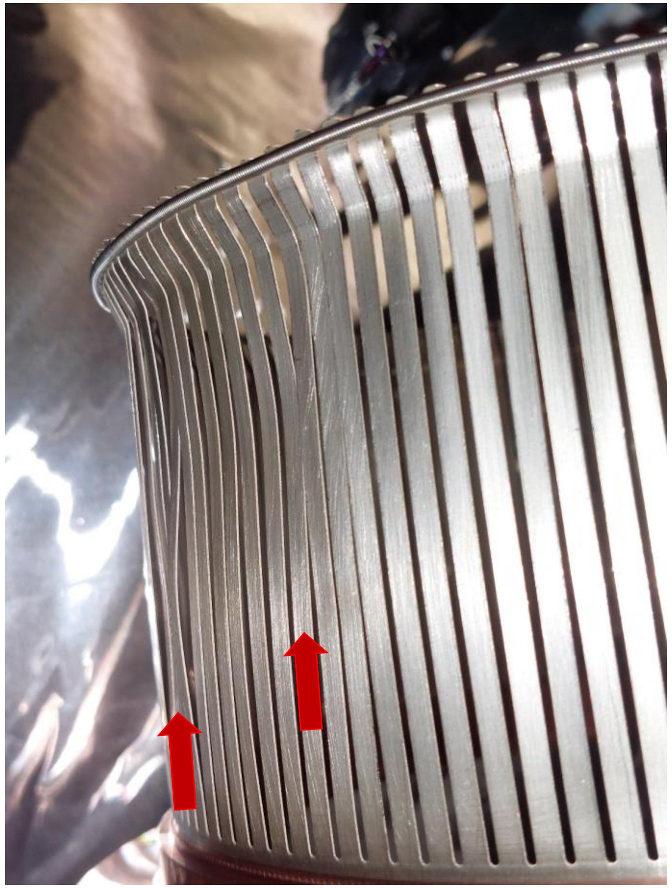

Pictures of VMBGA.A5R4.B

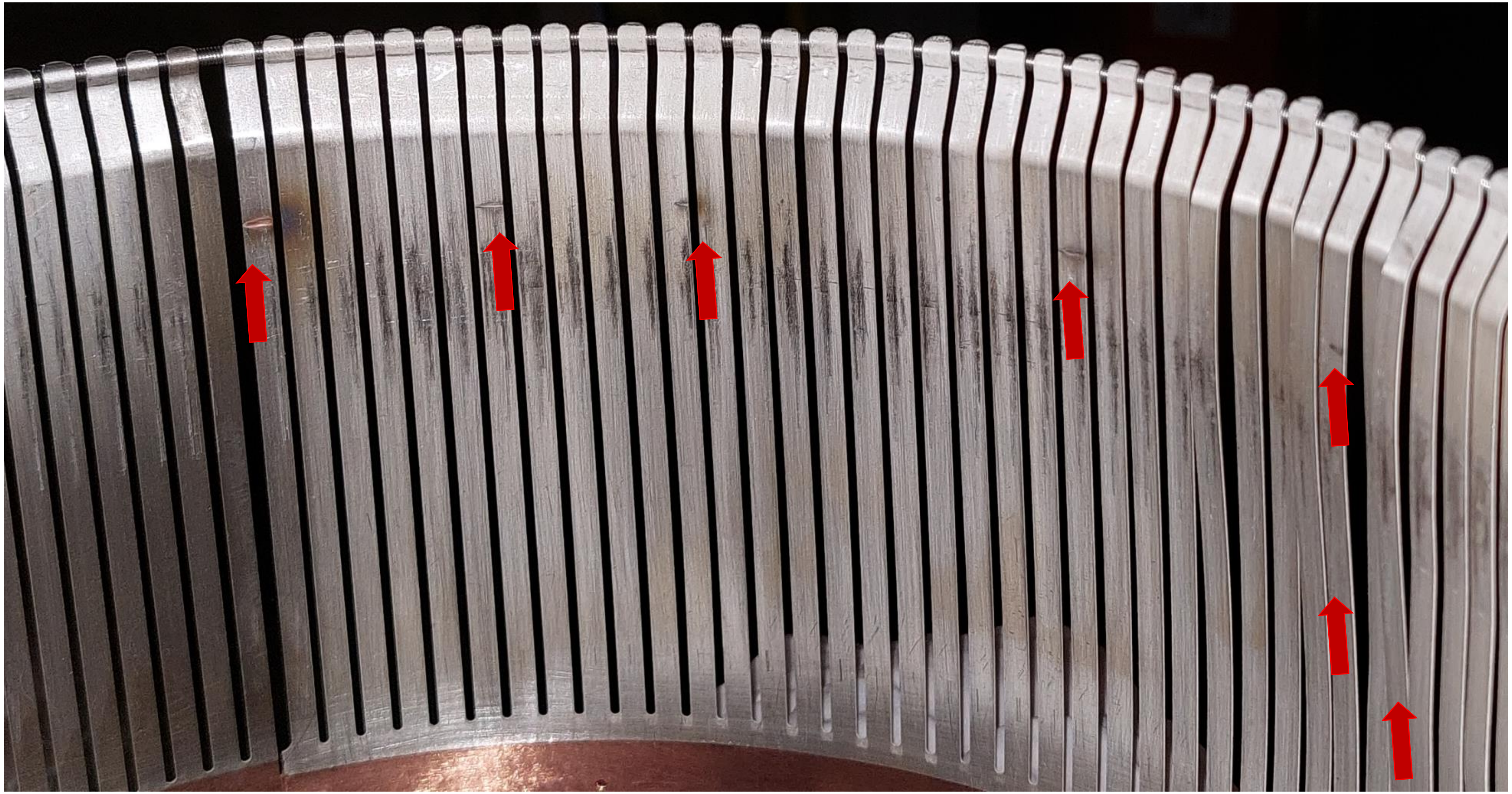

Module 5 RF & Insert with new and old spring

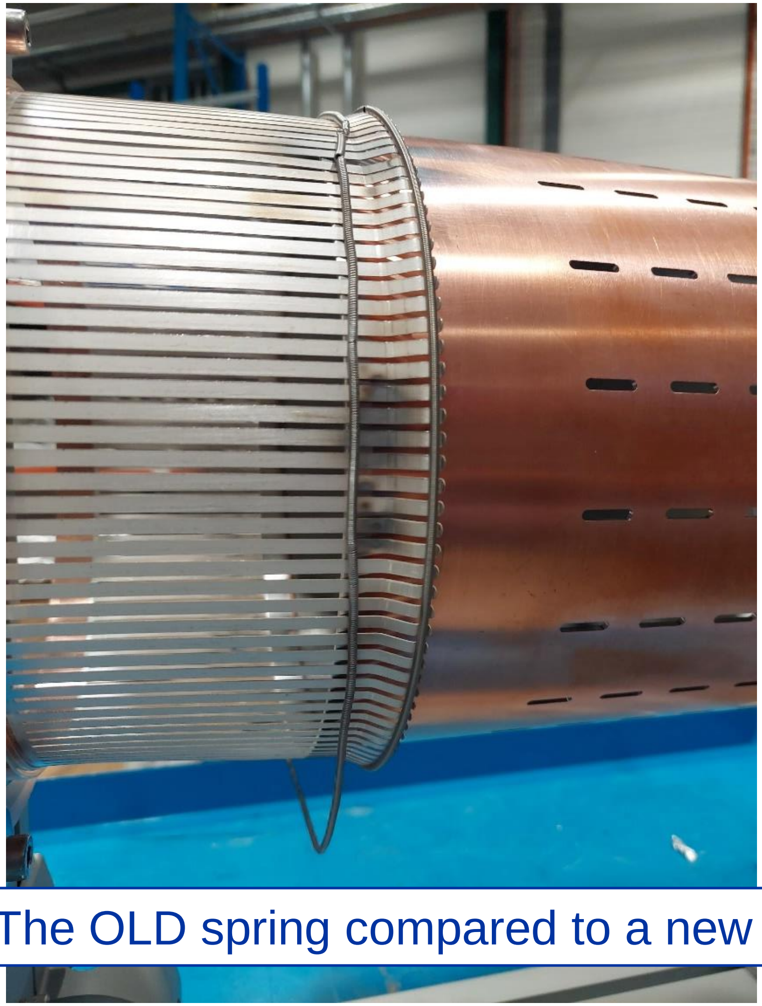

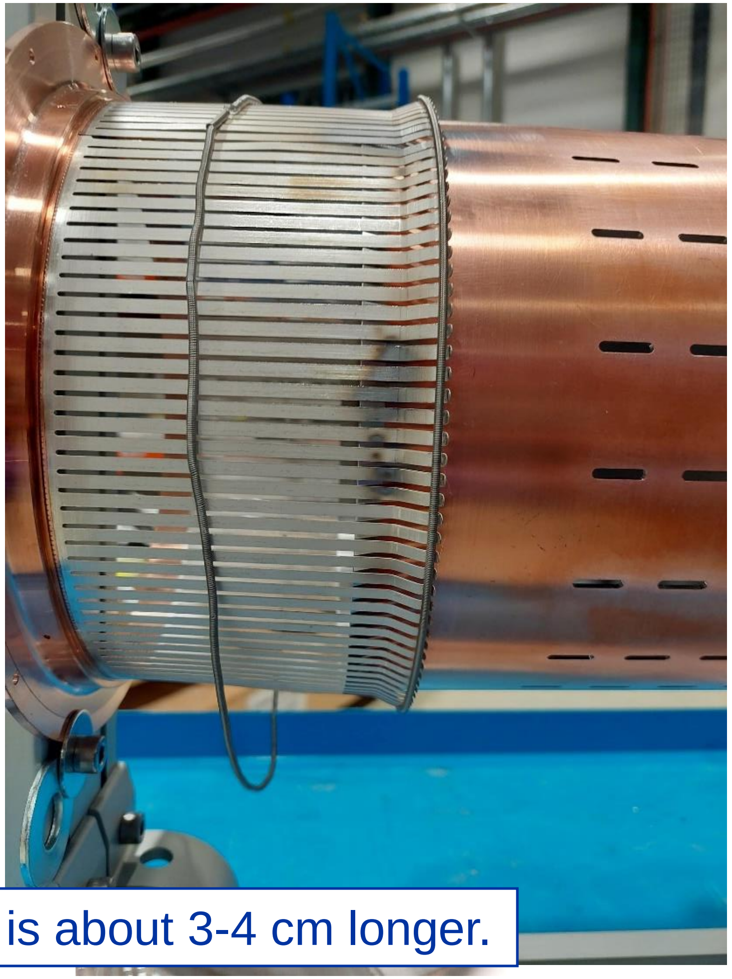

The OLD spring compared to a new one is about 3-4 cm longer.